ORGANOMETALLICS

Article

pubs.acs.org/Organometallics

Selective Hydrogenation of Amides to Amines and Alcohols Catalyzed by Improved Iron Pincer Complexes

Felix Schneck,[†] Maik Assmann,[†] Markus Balmer,[†] Klaus Harms,[†] and Robert Langer*[,†,‡]

[†]Department of Chemistry, Philipps-University Marburg, Hans-Meerwein-Straße, 35032 Marburg, Germany

[‡]Lehn Institute of Functional Materials (LIFM), Sun Yat-Sen University (SYSU), Xingang Road West, Guangzhou 510275, PR China

Supporting Information

ABSTRACT: A comparative study on the synthesis, stability, and catalytic activity of various iron pincer complexes with the general formula [(R-PN^{H}P)Fe(H) (CO) (BH_4)] is reported, where R denotes the substituent of the terminal PR_2-groups (R = ^{t}Bu, Cy, ^{i}Pr, Ph, Et). By the example of the synthesized precatalysts, it is shown that the nature of the ligands has a surprising influence on the catalytic properties of the complexes. Bulky ligands and less electron donating ligands affect the stability of the complexes, which preferably react under the loss of CO or H_2 to deactivated products. In return, the reduced steric demand and the strong σ-donating properties of the Et-substituted precatalyst (**2a**) lead to an improved activity in the hydrogenation of esters to alcohols, compared to that of the previously reported ^{i}Pr-substituted complexes. The improved activity of complex **2a** is clearly demonstrated in the direct hydrogenation of amides to alcohols and amines under mild conditions.

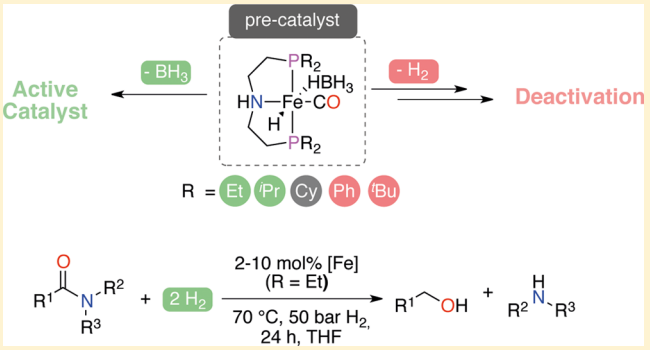

INTRODUCTION

Most industrial processes based on homogeneous catalysis use noble metals.[1] As these metals are expensive, often toxic, and not very abundant, the replacement by base metals is highly attractive. Complexes of pincer type ligands have shown high potential in catalytic reactions and after decades of intensive investigation they are still subject to ongoing research. In cases where they react in a noninnocent or cooperative way, these complexes can enable the activation of small molecules without changing the metal's formal oxidation state.[2−8] This makes them an ideal ligand platform for the development of earth-abundant metal-based catalytic systems. Especially pincer ligands of the combination PEP (E = C, N) are popular due to the ability to tune the electronic and steric features of the complex by simple variation of the substituents on the phosphorus atoms. With these ligands, significant progress has been made by evaluating iron(II) as catalyst for (de)hydrogenation reactions, for which the higher homologue ruthenium(II) shows excellent activity.[9−30] The pyridine-bisphosphine ligated iron(II) system by *Milstein* and co-workers is a great example of an iron(II) catalyst containing a PN^{Py}P-ligand, which is capable of catalyzing the hydrogenation and dehydrogenation of various substrates under mild conditions in high yield (Scheme 1).[31−36] Aside from the great catalytic activity, this system impressively illustrates the influence of minor ligand variations on the complexes' reactivity. While for the ^{i}Pr-substituted complex **A**, a dihydride species is not isolable and does not seem to be an intermediate of the catalytic cycle during ketone hydrogenation,[32,33] the dihydride species **B** is isolable due to bulkier ^{t}Bu-groups at the P donors. As a consequence, CO_2 and fluorinated esters can be hydrogenated with the *trans*-dihydride precatalyst.[31,34−36]

A second example of catalyst-tuning by small variations in the ligand manifold is the POCOP-based iron(II) catalyst **C** reported by Guan et al.[37,38] In this case, the catalytic activity of complex **C** in the dehydrogenation of ammonia borane was significantly increased by variation of the ancillary ligands and the substitution pattern at the central phenyl ring. As one ancillary phosphine ligand has to dissociate prior to substrate binding, an electron donating methoxy group has been introduced at the aryl backbone to accelerate the generation of a vacant coordination site. This modification in combination with the reduced donor properties of the ancillary phosphane ligands led to the more active catalyst **D**.

Very recently, different iron(II) (pre)catalysts with an amine-based PN^{H}P-pincer ligand were reported to exhibit excellent catalytic activity in different (de)hydrogenation reactions.[16−23,25−28] The group of Beller, for example, initially demonstrated high catalytic activity of [(^{i}Pr-PN^{H}P)Fe(H) (CO)(η^1-BH_4)] in the dehydrogenation of methanol−water mixtures to carbon dioxide and hydrogen.[16] Shortly afterward, the groups of Hazari, Schneider, and Jones reported about the dehydrogenation of formic acid as well as the dehydrogenation of primary and secondary alcohols to esters or ketones, respectively.[18,19,22] A potential hydrogen storage system using

Received: March 30, 2016

DOI: 10.1021/acs.organomet.6b00251
Organometallics XXXX, XXX, XXX−XXX

Scheme 1. Development of Iron Catalysts by *Milstein* and *Guan* Based on Rational Variation

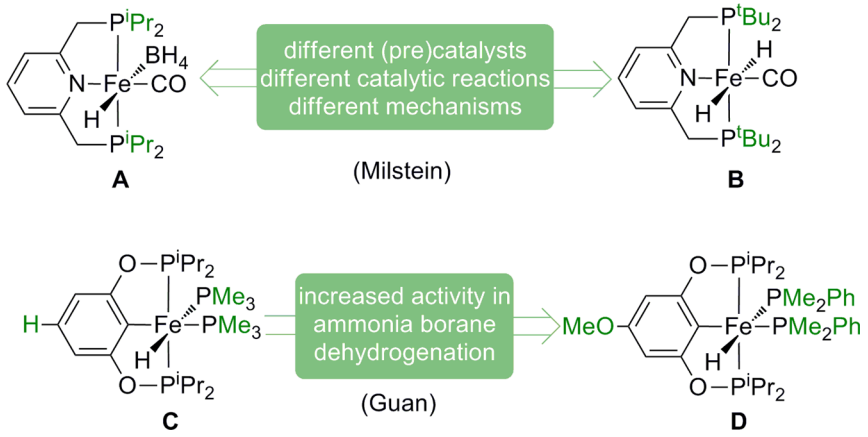

Scheme 2. Key-Intermediates within a Possible Catalytic Cycle

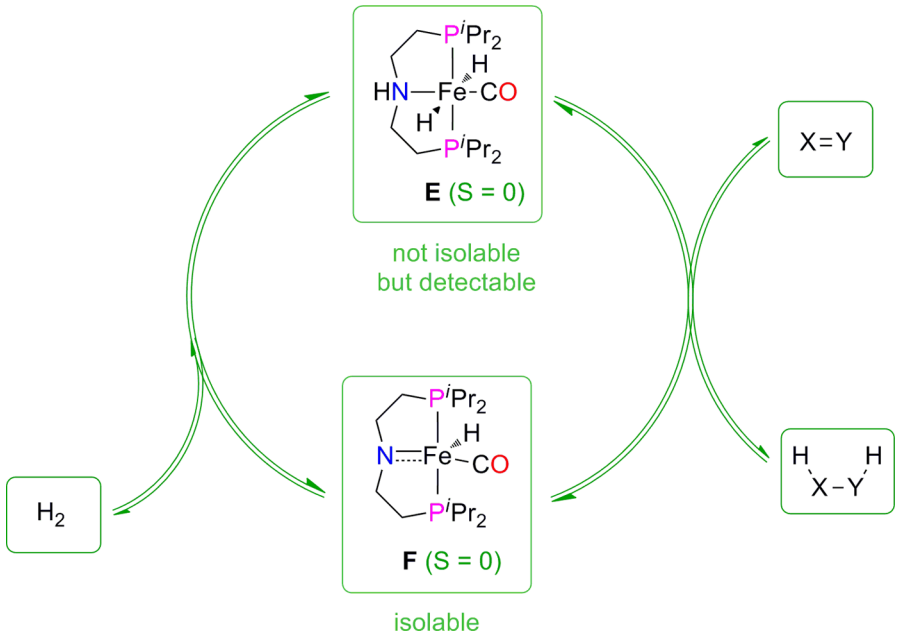

1,2,3,4-tetrahydroquinaldine as liquid organic carrier and these complexes as catalysts has been described by Jones and co-workers.[20] In parallel, the group of Beller reported the high catalytic activity of these complexes in the hydrogenation of nonactivated esters to alcohols.[27] Shortly afterward, the groups of Guan and Fairweather employed these complexes for the hydrogenation of fatty acid esters in the absence of solvent.[21,23]

Among the known iron-based hydrogenation catalysts for carbonyl compounds, this class of complexes with PN^{H}P-type ligands clearly exhibits the highest catalytic activity so far. The catalytic cycle likely involves complexes **E** and **F** as intermediates, which both exhibit a singlet ground state,[20] thus avoiding additional barriers due to system crossing between different spin states, which are often encountered for elementary steps with iron complexes (Scheme 2).[39,40] In particular, the singlet ground state of the square pyramidal complex **F** (τ = 0.22)[41] is remarkable, and as for iron(II) complexes with d^6 electron count and square pyramidal coordination geometry, spin states of S = 0, 1, and 2 are possible. As homogeneous iron catalysts are generally very sensitive to small variations of ligand and reaction parameters, the investigation of steric and electronic ligand effects in this system is a promising approach for catalyst improvement.

Herein, we present our results on the synthesis and stability of hydridoborohydride precatalysts [(R-PN^{H}P)Fe(H)(CO)-(η^1-BH$_4$)] (R = Et, ^{i}Pr, Cy, Ph, ^{t}Bu). Depending on the group R, different pathways for activation and decomposition are viable. On the basis of these results, a catalyst with an improved activity in the hydrogenation of esters to alcohols is reported. The same complex exhibits catalytic activity in the unprecedented iron-catalyzed hydrogenation of amides to alcohols and amines.

RESULTS

Synthesis of Hydridoborohydride Complexes. Inspired by the improvement of Milstein's and Guan's catalysts by fine-tuning the electronic and steric properties,[31−33,38] we were interested in the influence of the substituents R at the phosphorus donor groups in the amine-based R-PN^{H}P ligand (R-PN^{H}P = (R$_2$PCH$_2$CH$_2$)$_2$NH). The synthesis of the ^{i}Pr-PN^{H}P-based pincer-iron-complex **2b** was first reported by Beller and co-workers,[16] adopting a synthetic procedure

DOI: 10.1021/acs.organomet.6b00251
Organometallics XXXX, XXX, XXX−XXX

Scheme 3. Synthetic Route to [(R-PN^{H}P)Fe(X)$_2$(CO)] and [(R-PN^{H}P)Fe(H) (CO)(η^1-BH$_4$)] Complexes (X = Cl, Br)

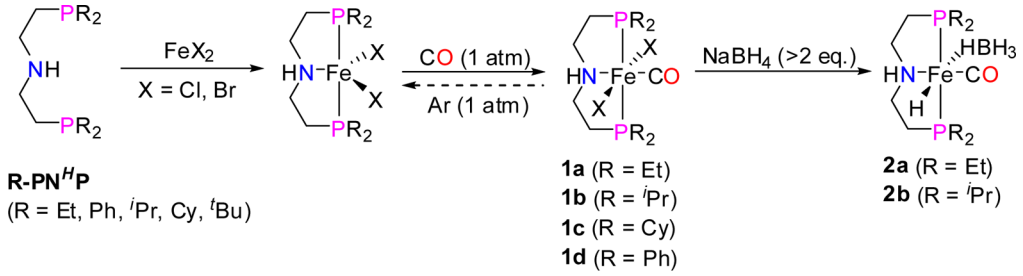

Scheme 4. Alternative Synthetic Route to the Desired [(R-PN^{H}P)Fe(H) (CO)(η^1-BH$_4$)] Complexes

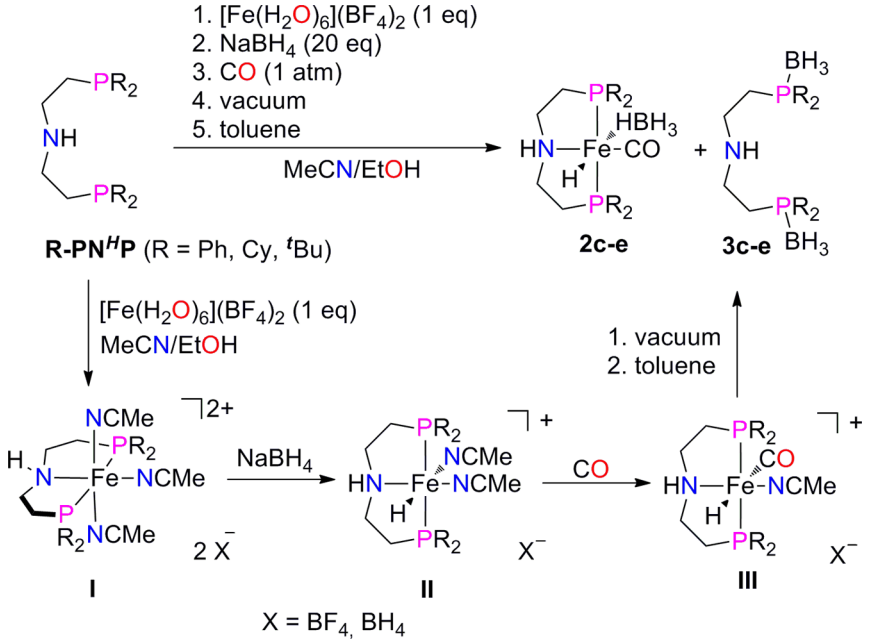

originally reported for the corresponding pyridine-based pincer complex **A** with ^{i}Pr-groups.[32] The desired complex was obtained in good yields by complexation of $FeBr_2$, followed by subsequent reaction with CO. Treatment of the resulting *trans*-dihalide carbonyl complex [(^{i}Pr-PN^{H}P)Fe(Br)$_2$(CO)] with excess $NaBH_4$ results in the formation of the desired complex. Attempts to prepare derivatives of these complexes with different substituents on the P donor groups were done by the group of Schneider and Hazari.[42] Thereby, [(Cy-PN^{H}P)-Fe(Cl)$_2$] has been reported to react with CO, but the subsequent reaction of [(Cy-PN^{H}P)Fe(Cl)$_2$(CO)] with $NaBH_4$ is described as unselective. The analogous synthesis of the ^{t}Bu-PN^{H}P-based compound failed due to a lack in reactivity of the dihalide precursor toward CO. As with bulky PN^{H}P-ligands, the corresponding hydridoborohydride complexes were not accessible via this route, and we started to investigate the less bulky Et-substituted ligand as well as the more electron-poor Ph-substituted ligand (Scheme 3).

The complexation of one equivalent of iron(II) halide in THF usually takes place with all ligands, as evident from the formation of a colored solution and the absence of a resonance for the uncoordinated ligand in the ^{31}P{^{1}H} NMR spectrum. On the basis of these findings, we assumed the formation of [(*R*-PN^{H}P)FeX$_2$].[43] Especially, for the less bulky ligand Et-PN^{H}P it is important to note that the ligand still exhibits enough steric demand to avoid 2-fold coordination and formation of [(Et-PN^{H}P)$_2$Fe](FeX$_4$), as observed for bipyridine-based PNN-type ligands.[44,45] Apart from ^{t}Bu-PN^{H}P, all dihalide complexes react with carbon monoxide to give the diamagnetic complexes **1a**–**d**. With the dialkylphosphino-containing ligands this reaction leads to stable *trans*-dibromo complexes **1a**–**c**, which can be isolated in good yields.[21,42] Furthermore, the molecular structure of the newly synthesized complex **1a** and **1d** have been confirmed by single crystal X-ray diffraction. The reaction with the Ph-substituted ligand, however, results in a mixture of the *cis*- and *trans*-dibromo carbonyl complex **1d**. Interestingly, the *cis*- and *trans*-complex **1d** turned out to liberate carbon monoxide in the absence of carbon monoxide atmosphere. Because of the limited stability of complex **1d**, it was not possible to prepare the corresponding hydridoborohydride complex by the addition of $NaBH_4$. A similar observation has been made with complex **1c**, which has been reported to react with $NaBH_4$ to an inseparable mixture of products. Only the reaction of complex **1a** with $NaBH_4$ results in the formation of the corresponding hydridoborohydride complex **2a**, as previously reported for **1b** and analogous pyridine-based pincer complexes.[16,32]

As the synthetic route described in Scheme 3 yields the desired hydride complex only in the case of the Et- and the ^{i}Pr-ligand, we followed a different approach that originally has been reported for the synthesis of the *trans*-dihydride complex **B**.[31] This procedure takes advantage of the selective reaction of the

DOI: 10.1021/acs.organomet.6b00251
Organometallics XXXX, XXX, XXX−XXX

Table 1. Spectroscopic Data for [(R-PN^{H}P)Fe(H) (CO) (BH_4)] (2a−e)

complex	R =	$\tilde{\nu}_{CO}$ (cm^{-1})	δ_H(Fe-*H*) (ppm)	$\delta_H(\eta^1\text{-}BH_4)$ (ppm)	δ_P(Fe-*P*) (ppm)	$\delta_B(\eta^1\text{-}BH_4)$ (ppm)
2a	Et	1892	−19.66 ($^2J_{PH}$ = 49.0 Hz)	−3.07	82.1	−32.9
2b[a]	^{i}Pr	1892/1833	−19.51/−20.18 ($^2J_{PH}$ = 50.0 Hz)	−2.84	99.5/100.9	−33.9
2c	Cy	1900	−19.59 ($^2J_{PH}$ = 50.4 Hz)	−2.84	91.9	−31.4
2d	Ph	n. a.	−18.13 ($^2J_{PH}$ = 52.3 Hz)	−3.61	81.7	−32.9
2e	^{t}Bu	n. a.	−20.83 ($^2J_{PH}$ = 60.4 Hz)	−2.05	111.0	−40.6

[a]Spectroscopic data have been taken from ref 16.

Scheme 5. Solution Behavior of Complexes 2a−e, Indicating Activation and Deactivation Pathways

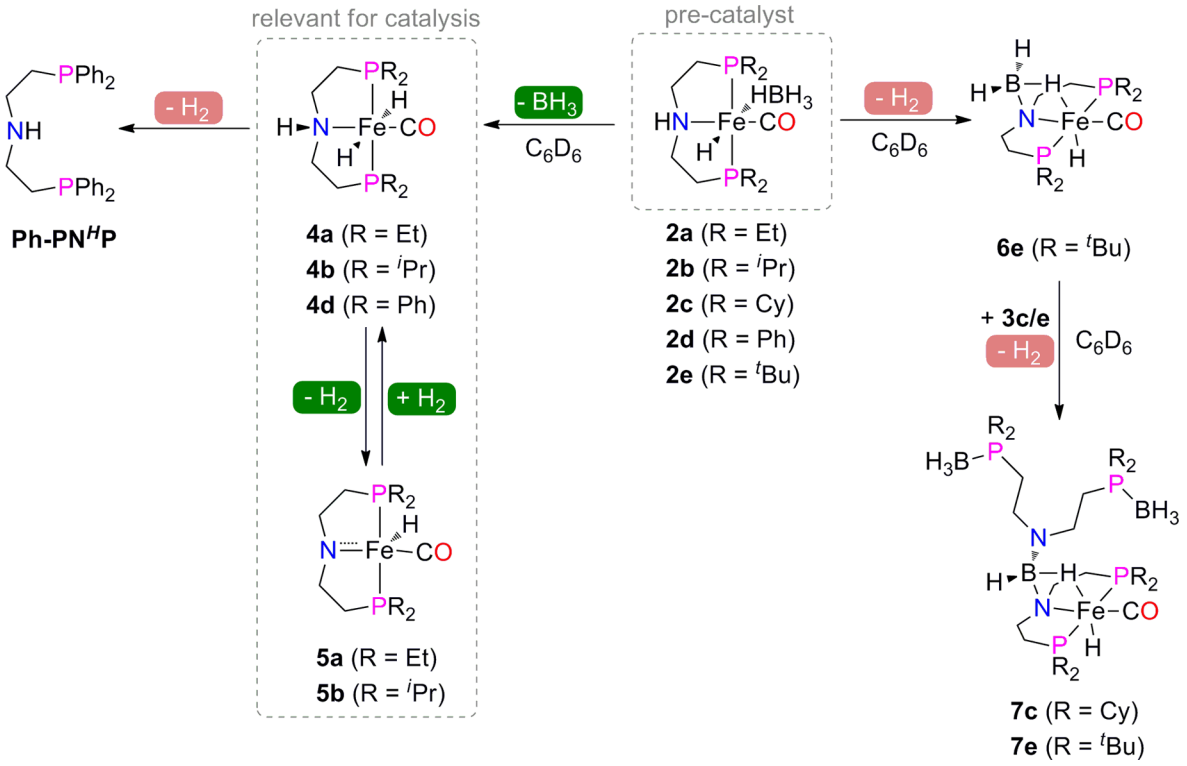

dicationic acetonitrile complex **I** (δ_p = 55.5 ppm, R = Cy) with $NaBH_4$ to give the cationic hydrido acetonitrile complex **II** (δ_p = 80.1 ppm, R = Cy, Scheme 4). Under 1 atm of CO, one MeCN ligand is replaced by a CO ligand, yielding the cationic hydrido carbonyl acetonitrile complex **III** (δ_p = 89.0 ppm, R = Cy). Continuous drying under high vacuum of this complex results in the loss of the remaining MeCN ligand and coordination of the BH_4-counterion to give hydridoborohydride complexes **2**. In the present case, the intermediate compounds **I**−**III** were not isolated, but subsequent analysis of the reaction mixture by $^{31}P\{^1H\}$ NMR spectroscopy shows selective reactions upon addition of the reactants.

For the extraction of the neutral complexes, **2** toluene was used to prevent BH_3 abstraction. The new complex **2c** is obtained in 31% yield, while the borane-substituted ligand **3c** is obtained as side-product.[46] **3c** is observable by $^{31}P\{^1H\}$ NMR spectroscopy after the addition of $NaBH_4$, suggesting an unselective reaction of the dicationic intermediate **I** with $NaBH_4$ that results in the desired monocationic hydrido complex **II** and another unstable intermediate, which decomposes under the formation of **3c**. Applying the same procedure with Ph-PN^{H}P and ^{t}Bu-PN^{H}P as ligands, the desired hydridoborohydride complexes **2d** and **2e** accompanied by the phosphinoboranes **3d** and **3e** could be observed by NMR spectroscopy, respectively, but the complexes are too unstable to allow for isolation or separation. Selected values from NMR and IR spectroscopic measurements are summarized in Table 1.

As previously reported for complex **2b**,[82] a mixture of two isomers is initially formed in the case of complex **2a**. The mixture of two isomers, differing in the relative orientation of N- and Fe-bound H atoms is slowly converted in solution to the thermodynamic stable complex with a *trans*-orientation of these two H atoms. All hydridoborohydride complexes (**2a−e**) give rise to a singlet resonance in the $^{31}P\{^1H\}$ NMR spectrum, ranging from 81.7 and 82.1 ppm for **2a** and **2d**, respectively, to a low-field shifted resonance at 111.0 ppm for complex **2e** with the bulkiest ligand. The ^1H NMR spectra of **2a−e** exhibit typical triplet resonances between −18.13 and −20.83 ppm for the hydrido ligands ($^2J_{PH}$ = 49.0−60.4 Hz), indicating a meridional coordination of the pincer ligands with magnetically equivalent phosphorus atoms. The broad resonances between −2.05 and −3.61 with an integral of four in the ^1H NMR spectrum suggest the presence of an η^1-coordinated BH_4-ligand.[16,21,47,48] For complexes **2a−2d**, the isomer with a close proximity between the BH_4-ligand and the NH-proton was found to be the more stable one, as judged by ^1H NOESY NMR spectroscopy. For complexes **2a−d**, broad resonances between −31.4 and −33.9 ppm are observed in the $^{11}B\{^1H\}$

DOI: 10.1021/acs.organomet.6b00251
Organometallics XXXX, XXX, XXX−XXX

Scheme 6. Dehydrogenation of the Borane Adduct 3c in the Presence of 7c

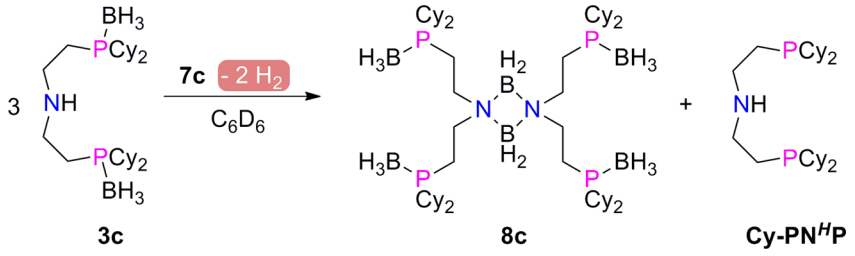

NMR spectra, whereas complex **2e** gives rise to a broad resonance at −40.6 ppm, which might indicate a more weakly bound BH_4-ligand due to steric repulsion. Because of the continuous presence of decomposition products in samples of **2d** and **2e**, it was not possible to unambiguously assign the CO-stretching vibration in the acquired FT-IR spectra. Nonetheless, for **2a** and **2b** equal wavenumbers of $\tilde{\nu}_{CO}$ = 1892 cm^{-1} were observed for the corresponding *trans*-isomer in the FT-IR spectrum, whereas complex **2c** shows a slightly shifted band at 1900 cm^{-1}. Although the C−O-vibration is usually coupled to the Fe−H-vibration in such cases, the shifted band suggests a weaker π-backbonding in **2c** with respect to **2a** and **2b**.

Activation and Decomposition Pathways of 2a−e. For the hydridoborohydride complex **2b**, it has been previously demonstrated that this complex reacts under loss of BH_3 upon heating or treatment with a Lewis base to give a mixture of the *trans*-dihydride complex **4b** and the *penta*-coordinated amido complex **5b**.[21] The Et-substituted precatalyst **2a** exhibits a very similar reactivity in a solution of aprotic solvent such as benzene, toluene, or THF (Scheme 5). The analogous *trans*-dihydride complex *trans*-**4a** gives rise to a multiplet resonance at −9.66 ppm in the ^{1}H NMR spectrum for the two hydrido ligands in *trans*-**4a**. A singlet resonance at 93.1 ppm in the $^{31}P\{^1H\}$ NMR spectrum is assigned to *trans*-**4a**. Interestingly, minor quantities of the corresponding *cis*-dihydride *cis*-**4a** can be detected when **2a** is treated with a BH_3-acceptor such as PEt_3, as judged by the appearance of two triplet of doublet resonances at −20.00 ppm ($^2J_{PH}$ = 51.3 Hz, $^2J_{HH}$ = 14.2 Hz) and −8.06 ppm ($^2J_{PH}$ = 85.2 Hz, $^2J_{HH}$ = 14.9 Hz). The hydride ligand in complex **5a** gives rise to a high-field shifted triplet resonance at −24.40 ppm ($^2J_{PH}$ = 50.9 Hz) in the ^{1}H NMR spectrum. The phenyl-substituted complex **2d** turns out to be much less stable in solution than its Et- and ^{i}Pr-counterparts **2a** and **2b**. In the ^{1}H NMR spectrum of **2d** or mixtures of **2d** and **3d**, usually a significant amount of H_2 is detected. Because of the limited lifetime of **2d**, a mixture of **2d** and **3d**, was analyzed by multinuclear NMR spectroscopy. The $^{31}P\{^1H\}$ NMR spectrum after a couple of hours exhibits several new singlet resonances between 75 and 100 ppm, as well as a singlet resonance at −18.6 ppm, corresponding to the free ligand Ph-PN^{H}P. Only small quantities of the initial hydridoborohydride complex **2d** were detectable by ^{1}H and $^{31}P\{^1H\}$ NMR spectroscopy. The major species in solution at this time exhibits a singlet resonance at 94.4 ppm in the $^{31}P\{^1H\}$ NMR spectrum as well as a resonance with an integral of two at −8.42 ppm in the ^{1}H NMR spectrum. A careful analysis revealed that these signal consists of two superimposed triplet of doublet resonances at −8.42 ppm ($^2J_{PH}$ = 67.0 Hz, $^2J_{HH}$ = 10.5 Hz) and −8.41 ppm ($^2J_{PH}$ = 63.1 Hz, $^2J_{HH}$ = 9.7 Hz). Such multiplicity is in line with a *trans*-dihydride complex **4d**, in which the two hydrido ligands are magnetically nonequivalent, due to a different relative orientation to the NH-proton. Nonetheless, complex **2d** decomposes within 1 day to unidentified products and the Ph-PN^{H}P. As the dibromo complex **1d** was labile toward the liberation of the carbonyl ligand, such a pathway might be viable for the hydridoborohydride complex **2d** as well and would explain the distinct instability.

Complexes **2c** and **2e** exhibit only limited stability in solution too, as evident from a continuous decrease of the resonances corresponding to hydride and the BH_4 ligand and concomitant formation of H_2 in the ^{1}H NMR spectrum. Interestingly, in the presence of a Lewis base such as THF, which has been used as BH_3-acceptor for analogous complexes with a pyridine-based pincer ligand,[31] no BH_3-transfer is detected. Such a transfer would lead to the assumed active species **E** or **F**. However, in the presence of the ligand borane adduct **3c**/**e** the selective formation of complex **7c**/**e** can be observed (Scheme 6). These complexes give rise to an AB spin system centered at 97.9 and 118.2 ppm as well as a broad resonance in the $^{31}P\{^1H\}$ NMR spectrum with an almost identical chemical shift like the borane adducts **3c**/**e**. The ^{1}H NMR spectrum of **7c** exhibits a virtual triplet of doublet at −14.60 ppm ($^2J_{PH}$ = 59.5 Hz, $^2J_{HH}$ = 4.5 Hz) for the hydrido ligand, which simplifies to doublet resonance upon ^{31}P-decoupling. Instead of the four proton resonance corresponding to the coordinated BH_4-ligand in complex **2c**, a broad resonance at −11.17 ppm that integrates to one is observed in the ^{1}H NMR spectrum of **7c**. Complex **7e** give rise to a triplet of doublets at −14.93 ppm for the hydride ligand ($^2J_{PH}$ = 59.4 Hz, $^2J_{HH}$ = 4.2 Hz) and a broad one proton resonance at −9.65 ppm for the bridging boron-bound hydrogen atom in the ^{1}H NMR spectrum. The resonance of the terminal B−H-proton in **7c** is observed at 3.19 ppm in the ^{1}H NMR spectrum, whereas the resonance of the two BH_3-groups is only assignable upon ^{11}B-decoupling, resulting in a well resolved doublet resonance ($^2J_{PH}$ = 14.3 Hz). Two broad resonances at −11.8 and −42.6 ppm are observed in the $^{11}B\{^1H\}$ NMR spectrum of **7c**, corresponding to the N-BH_2-N-bound boron atom and the phosphorus bound BH_3-groups. Very similar values of −11.9 and −42.3 ppm are observed in the $^{11}B\{^1H\}$ NMR spectrum of complex **7e**. In case of the ^{t}Bu-substituted ligand, an intermediate could be observed by ^{1}H, $^{31}P\{^1H\}$, and $^{11}B\{^1H\}$ NMR spectroscopy, which slowly converts to **7e** and other unidentified products. The hydrido ligand in complex **6e** gives rise to a triplet resonance at −15.85 ppm ($^2J_{PH}$ = 63.4 Hz), whereas a broad resonance at −10.29 ppm in the ^{1}H NMR spectrum indicates a coordinating B−H group, similar to those in **7c**/**e**. The appearance of a singlet resonance at 103.7 ppm in the $^{31}P\{^1H\}$ NMR spectrum suggests a symmetric complex with two magnetically equivalent phosphorus atoms, while the broad resonance at −21.9 ppm in the $^{11}B\{^1H\}$ NMR spectrum indicates a different environment of the boron atom in **6e** in comparison to those of **7c** and **7e**. On the basis of the spectroscopic data, it is assumed that

DOI: 10.1021/acs.organomet.6b00251
Organometallics XXXX, XXX, XXX−XXX

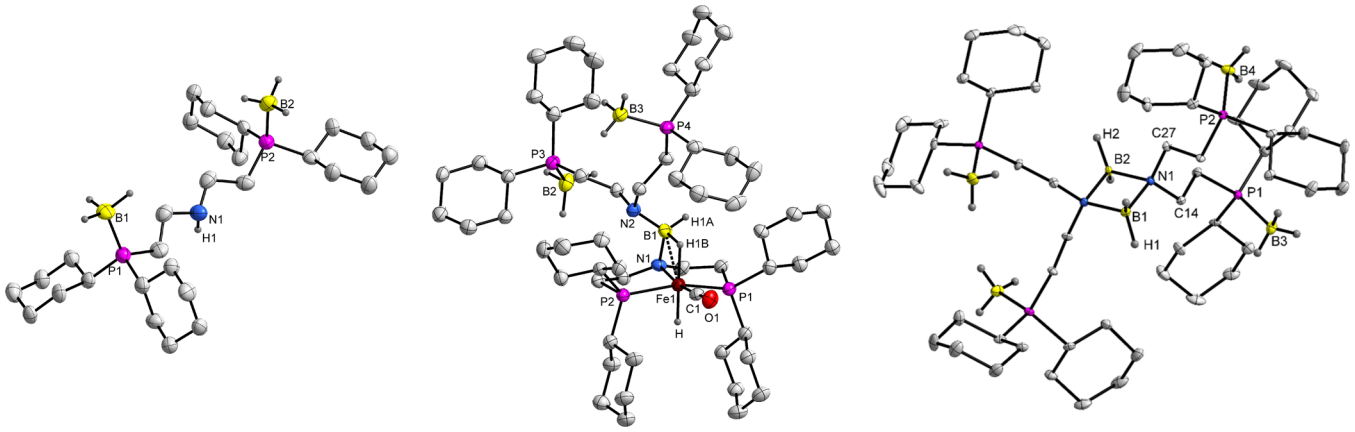

Figure 1. Molecular structure of **3c** (left), **7c** (middle), and **8c** (right) in the crystal lattice with ellipsoids set to 50% probability (carbon bound hydrogen atoms were omitted for clarity).

complex **6** is the initial product of the first H_2-elimination step. As in all hydridoborohydride complexes **2a**–**d**, the isomer with the N–H-proton and the BH_4-ligand on the same site of the complex is found to be the more stable one, and the dehydrogenation step likely proceeds via the protonation of the coordinated BH_4-ligand in **2c**/**e**, consecutive H_2-elimination, and B–N-bond formation.

Finally, the molecular structure of complex **7c** was confirmed by single crystal X-ray diffraction (Figure 1). The central iron(II) atom in **7c** remains octahedrally coordinated by the two dicyclohexylphosphino donor groups and the central nitrogen atom as well as a hydride and a carbonyl ligand. During the reaction with the borane-bound ligand **3c**, a rare M–N–B-H borametallacycle has been formed.[49−53]

The BH_2-fragment likely originates from the coordinated BH_4-ligand in **2c**, which subsequently forms H_2 by the reaction with an amine proton. Interestingly, the band at 1891 cm^{-1} corresponding to the C–O stretching vibration in the FT-IR spectrum is shifted toward lower wavenumbers in comparison to those of **2c**, indicative of a stronger π-back bonding from the central iron atom. If a solution of complex **7c** and additional borane adduct **2c** is allowed to stand at ambient temperature for 2 or 3 weeks, the formation of colorless crystals can be observed. The $^{31}P\{^1H\}$ and $^{11}B\{^1H\}$ NMR spectra of these crystals appears almost identical to those of **3c**, but the single crystal X-ray diffraction analysis of these crystals shows that compound **3c** gets slowly dehydrogenated to the dimeric B_2N_2-cycle **8c** in the presence of complex **7c** (Figure 1). Such dimerization reactions have been previously observed with other ammonia boranes such as Me_2NH-BH_3, MePhNH-BH_3, or $(CH_2)_4NH$-BH_3 in the presence of transition metal complexes.[54−58] The analysis of the supernatant solution confirmed concomitant formation of free ligand Cy-PN^{H}P, indicating a BH_3-group transfer in this dehydrogenation reaction.

As complex **2c** undergoes a dehydrogenative coupling with the borane protected ligand **3c**, it seems likely that **2c** reacts with other primary or secondary amines as well. For this reason, we investigated the reactivity of **2c** toward aniline, which has been previously used as a BH_3-acceptor with borohydride complexes.[32] As the dehydrocoupling reaction with **3c** appears to be rather slow, the sample was heated to 50 °C and continuously analyzed by NMR spectroscopy. With 2.2 equiv of aniline, the ^1H and $^{31}P\{^1H\}$ NMR spectra show the formation of a new main product (67%) in addition to complex **7c** (Scheme 7). The new complex **9c** gives rise to an AB spin system centered at 101.3 ppm in the $^{31}P\{^1H\}$ NMR spectrum

Scheme 7. Dehydrogenative Coupling of Aniline with Complex 2c

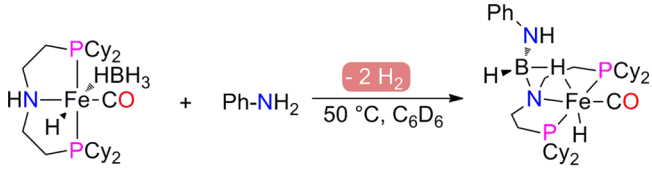

(J_{AB} = 118.6 Hz, $\Delta\nu$ = 199.7 Hz). A triplet resonance at −14.55 ppm ($^2J_{PH}$ = 59.2 Hz), which is superimposed with the triplet resonance at −14.60 ppm of **7c**, is observed for the hydride ligand in complex **9c**, whereas the coordinating B–H group gives rise to a broad one proton resonance at −10.49 ppm in the ^1H NMR spectrum.

For complexes **2a**, **2b**, and **2d**, it has been shown that they preferably release BH_3, either at ambient temperature (**2d**) or upon heating or treatment with a BH_3-acceptor (**2a**/**b**), to give a mixture of the *trans*-dihydride species **4** and the *penta*-coordinated species **5**.[21] As the hydrido borohydride complexes **2c** and **2e** with more bulky ligands preferably release H_2 in favor of the BH_3-release, we were investigating whether this pathway can be suppressed in the presence of hydrogen gas. In the case of complex **2c**, a decrease in intensity of the corresponding resonances and evolving signals for complexes **7c** and **9c** are still observed under 1 atm of hydrogen pressure by ^1H and $^{31}P\{^1H\}$ NMR spectroscopy. Only after approximately 90% of conversion of **2c**, a small amount of the *trans*-dihydride complex **5c** is detected by NMR spectroscopy.[18] This species gives rise to a resonance at −9.29 ppm in the ^1H NMR spectrum, which is best described as two superimposed triplet of doublet resonances ($^2J_{PH}$ = 40.2 Hz and $^2J_{HH}$ = 8.6 Hz for the first one and $^2J_{PH}$ = 40.8 Hz and $^2J_{HH}$ = 8.4 Hz for the second one). A singlet resonance at 105.6 ppm in the $^{31}P\{^1H\}$ NMR spectrum was assigned to this complex.

If a solution of complex **2e** is treated with 1 atm of H_2, a decrease in intensity is still observed, but **7e** is just formed to a minor extent. Instead, two broad resonances at −6.00 and −8.19 ppm with equal integrals exhibit increased intensities in the ^1H NMR spectrum ($\nu_{1/2}$ = 36.5 and 36.2 Hz). The former

DOI: 10.1021/acs.organomet.6b00251
Organometallics XXXX, XXX, XXX–XXX

resonance appears to be a broadened triplet with $^2J_{PH}$ = 43.1 Hz that simplifies to a singlet upon ^{31}P-decoupling. This species gives rise to a singlet resonance at 118.1 ppm in the $^{31}P\{^1H\}$ NMR spectrum, which again is broadened with respect to the resonances of **2e** and **6e**. The chemical shifts in the ^{1}H NMR spectrum allow one to propose a *trans*-arrangement of a hydride and a carbonyl ligand in this species (Scheme 8).

Scheme 8. Reactivity of Hydrido Borohydride Complex 2e under 1 atm of Hydrogen

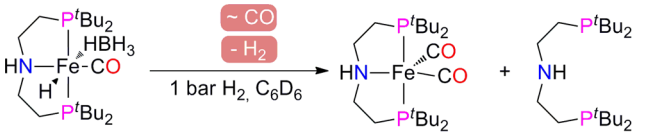

2e **10e** **^{t}Bu-PN^{H}P**

Because of the limited stability of this species, a further analysis was not possible. In addition, two high-field shifted triplet resonances at −25.43 ppm ($^2J_{PH}$ = 55.3 Hz) and −29.30 ppm ($^2J_{PH}$ = 51.8 Hz) can be located in the ^{1}H NMR spectrum. The strong high-field shift of these resonances and the absence of H−H-coupling are indicative of *penta*-coordinated amido complexes with a vacant coordination site *trans* to the hydrido ligand. Nonetheless, all attempts to isolate these complexes resulted in the formation of the iron(0)dicarbonyl complex **10e**. Such an intermolecular carbonyl ligand transfer of unsaturated iron hydride fragments has previously been observed for iron pincer complexes.[18,42]

The molecular structure of **10e** has been confirmed by single crystal X-ray diffraction (Figure 2). On the basis of the

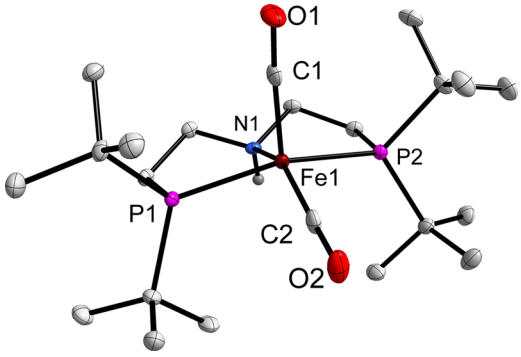

Figure 2. Molecular structure of **10e** in the crystal lattice with ellipsoids set to 50% probability (carbon bound hydrogen atoms were omitted for clarity).

parameter τ = 0.17, the coordination geometry of the central iron atom is best described as square pyramidal. Notably, the Fe−C−O angle of the apical carbonyl ligand in **10e** is significantly bent (168.1°), which has been previously observed for the analogous ^{i}Pr-substituted complex.[42] The infrared spectrum of solid complex **10e** showed several strong bands in the range of 1700 to 2100 cm^{-1}, which is in contrast to the assumption of a single species. A similar observation has been made by Goldmann and co-workers for the pyridine based complex [(^{t}Bu-PN^{Py}P)Fe(CO)$_2$], where this observation was attributed to dynamic behavior in solution.[59] In the present case, different relative orientations of the NH-proton are possible in addition to the two coordination geometries square pyramidal and trigonal bipyramidal. The two strongest bands are observed at 1760 and 1824 cm^{-1}, which is in good agreement with values reported for [(^{i}Pr-PN^{H}P)Fe(CO)$_2$].[42] Interestingly, the $^{31}P\{^1H\}$ NMR spectrum of **10e** in benzene-d_6 or toluene-d_8 does not show any resonance, whereas the ^{1}H NMR spectrum provides evidence for the presence of paramagnetic species.

Overall, the steric demand of the ligands has a strong impact on the stability of the synthesized precatalysts **2a**−**e**. In this comparative study, we were able to show that different pathways of activation are viable for iron hydrido borohydride complexes in solution. If the steric demand is too high, H_2 is preferably released rather than BH_3, leading to deactivated complexes. In a likewise manner, the phenyl-substituted complex **2d** in fact releases BH_3 to some extent but suffers from decomposition of the formed species that is too fast. On the basis of the gained information about the reactivity patterns of complexes **2a**−**e**, the complexes with sterically less demanding dialkylphosphino groups are expected to be the most active (pre)catalysts.

Catalytic Hydrogenation Reactions. Within this study, differences in stability and reactivity of the prepared hydrido borohydride complexes **2a**−**e** have been encountered, by simple change of the substituents of the phosphine donor groups. Next, we investigated the catalytic activity of sufficiently stable precatalysts **2a**, **2b**, and **2c** in the hydrogenation of different substrates and compared there activity with those of the previously reported precatalyst **2b**. As complex **2d** showed no activity in the hydrogenation of acetophenone to 1-phenylethanol, it has not been further investigated for the hydrogenation of more inert substrates. Complex **2b** exhibits excellent activity in the hydrogenation of the nonactivated ester methyl benzoate to benzyl alcohol and methanol (Table 2).[27]

Table 2. Hydrogenation of Methyl Benzoate Catalyzed by [(R-PN^{H}P)Fe(H) (CO) (BH$_4$)] (2a−c)[a]

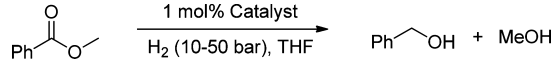

entry	complex	R =	p(H$_2$) (bar)	T (°C)	t (h)	conversion[b] (%)	yield[b] (%)
1	**2c**	Cy	10	100	6	52	46
2[c]	**2b**	^{i}Pr	10	100	6	91	88
3[c]	**2b**	^{i}Pr	50	100	6	99	93
4[c]	**2b**	^{i}Pr	50	80	6	87	82
5[c]	**2b**	^{i}Pr	50	60	6	52	49
6	**2a**	Et	10	60	6	68	62
7	**2a**	Et	10	70	6	89	89
8	**2a**	Et	10	100	6	32	23
9	**2a**	Et	50	70	6	96	95
10	**2a**	Et	50	100	6	>99	99

[a]Reaction conditions: methyl benzoate (0.5 mmol), precatalyst **1b**−**e** (0.005 mmol), and *m*-xylene (1.0 mmol) as internal standard and THF (1 mL). [b]Conversion and yield were determined by GC analysis using *m*-xylene as an internal standard. [c]Data have been taken from ref 27.

Using 1 mol % catalyst loading, complex **2b** showed the highest activity at 100 °C and 50 bar of hydrogen pressure, yielding 93.0% of the corresponding alcohols (entry 3). At lower hydrogen pressures (10 bar), the yield of benzyl alcohol and methanol is only slightly decreased to 88.0% (entry 2), whereas lowering the temperature results in a significant drop of activity, ranging from 82.0% yield at 80 °C (entry 4) to 49.0% yield at 60 °C (entry 5). Complex **2c** in comparison was only capable

DOI: 10.1021/acs.organomet.6b00251
Organometallics XXXX, XXX, XXX−XXX

Table 3. Hydrogenation of Amides Catalyzed by [(Et-PN^{H}P)Fe(H) (CO) (BH_4)] (2a)[a]

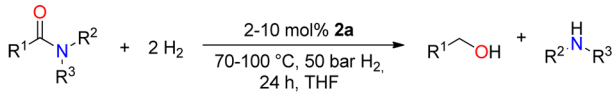

entry	amide	S/C	Temperature / °C	conversion[b] / %	alcohol (yield / %)	amine (yield / %)
1	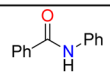	10/1	70	94	 90	 93
		50/1	70	57	45	45
		50/1	100	>99	99	99
2	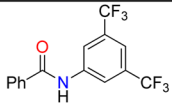	10/1	70	>99	 82	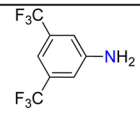 83
		50/1	70	57	53	53
3	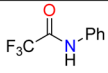	50/1	70	>99	 (n. d.)	99
4		10/1	70	0	 0	 (n. d.)
		10/1	100	14	4	(n. d.)
5		10/1	70	36	 14	 (n. d.)
		10/1	100	53	50	(n. d.)
6		10/1	70	0	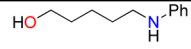 0	
		10/1	100	0	0	
7	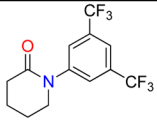	10/1	70	0	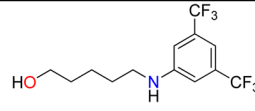 0	
		10/1	100	0	0	
8		10/1	70	0	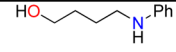 0	
		10/1	100	49	41[c]	
9	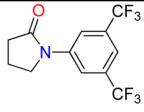	10/1	70	84	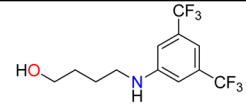 70[c]	
		10/1	100	>99	92[c]	

[a]Reaction conditions: substrate (1.00 mmol), precatalyst **2a** (0.02−0.10 mmol), and *m*-xylene (1.00 mmol) as internal standard and THF (5 mL). [b]Conversion and yield were determined by GC analysis using *m*-xylene as an internal standard. [c]Isolated yield.

of catalyzing the reaction with 46.5% yield at 100 °C and 10 bar of hydrogen pressure (entry 1). Applying the same conditions with complex **2a** gives even lower yields of 23.0% (entry 7). For this reason, we investigated the activity of complex **2a** at different temperatures with 10 bar hydrogen pressure (entries 6−8). Under low hydrogen pressure, complex **2a** exhibits a higher activity at 70 °C than at 100 °C (entry 7). Applying higher hydrogen pressures of 50 bar at 70 °C, complex **2a** catalyzes the hydrogenation of methyl benzoate to benzyl alcohol in 95.0% yield (entry 9). With 50 bar hydrogen pressure at 100 °C reaction temperature, full conversion and formation of benzyl alcohol in more than 99% is observed with complex **2a** as catalyst. In general, complex **2a** seems to be thermally less stable than **2b** at lower hydrogen pressures. As

DOI: 10.1021/acs.organomet.6b00251
Organometallics XXXX, XXX, XXX−XXX

complex **2a** and **2b** are very similar in spectroscopic properties, the reason for the higher activity in comparison to the reported value of **2b** is likely the reduced steric demand of the diethylphosphino-groups. This seems to result in lower steric repulsion between the catalyst and the substrate, thus lowering reaction barriers within the catalytic cycle rather than lowering the barriers of one of the discussed decomposition pathways.

On the basis of the catalytic activity in the hydrogenation of methyl benzoate, we chose complex **2a** as the most active catalyst to explore new substrates and extend the scope of the developed catalysts. Although much progress has been made in the homogeneous hydrogenation of esters to alcohols, very few examples for the significantly more difficult hydrogenation of amides have been reported, and no active iron-based catalyst is among those.[60−74] In particular, the hydrogenation of amides to alcohols and amines is desired, but with some of the reported catalysts, C−O-cleavage and therewith the formation of secondary amines are rather observed than C−N-cleavage.[62,70] This C−O-cleavage is a result of facile hemiaminal dehydration after the first reduction step of the amide and consecutive hydrogenation of the formed imine. According to DFT calculations, the C−N-cleavage is achieved by proton transfer from the ligand to the nitrogen atom of the O-bound aminal after the first reduction step, leading to amine-release and formation of the aldehyde-bound complex.[75]

Treatment of *N*-phenylbenzamide with H_2 (50 bar) at 70 °C in dry THF with a catalytic amount of **2a** (10 mol %) results in the clean formation of 90% benzylalcohol and 93% aniline after 24 h, whereas the secondary amine benzylphenylamine was not detected by GC analysis (Table 3, entry 1). If the catalyst loading is decreased to 2 mol % benzyl alcohol, then aniline is obtained in 45% yield. At 100 °C, benzyl alcohol and aniline are obtained in 99% yield. With *N*-(3,5-bis(trifluoromethyl)-phenyl)benzamide, complete hydrogenation to benzyl alcohol and 3,5-bis(trifluormethyl)aniline is observed (entry 2). The activated substrate trifluoracetanilide is completely hydrogenated to 2,2,2-trifluorethanol and aniline with even the lower catalyst loading of 2 mol % under otherwise identical conditions (entry 3). Interestingly, the hydrogenation of *N*-methylbenzamide proceeds only to a minor extent with complex **2a** as catalyst (entry 4), but the corresponding tertiary amide *N*,*N*-dimethylbenzamide undergoes hydrogenation with a modest yield of 50% (entry 5). *δ*-Lactams such as *N*-phenyl-2-piperidone (entry 6) and the more activated *N*-bis-(trifluoromethyl)phenyl-2-piperidone (entry 7) cannot be hydrogenated with complex **2a** as precatalyst. Nonetheless, the corresponding *γ*-lactams, *N*-phenyl-2-pyrrolidone and *N*-bis(trifluoromethyl)phenyl-2-pyrrolidone, are readily hydrogenated with complex **2a** as catalyst (entries 8 and 9). The resulting amino alcohols were isolated in yields of 41% and 92%.

In summary, complex **2a** represents an active precatalyst for the hydrogenation of different classes of nonactivated amides. More activated amides can get hydrogenated with only 2 mol % catalyst loading under even milder conditions, yielding the corresponding amines and alcohols with excellent selectivity.

CONCLUSIONS

In the current study, we demonstrated that minor changes in the ligand moiety of amine-based iron pincer complexes can have a strong impact on complex stability and reactivity patterns. With the synthesis of a series of possible precatalysts, we were able to observe different reaction pathways of these complexes in solution that finally allowed for the identification of the most suitable precatalyst. Accordingly, the complexes with the less bulky ethyl- and *iso*-propyl-groups showed sufficient stability and represent the most active hydrogenation catalysts. Furthermore, complex **2a** was utilized in the hydrogenation of amides to amines and alcohols, a reaction only a few ruthenium complexes are reported to be capable of catalyzing. Therewith, complex **2a** represents the first example of an iron-based catalyst for the hydrogenation of such a challenging type of substrate.[74]

EXPERIMENTAL SECTION

Materials and Methods. All experiments were carried out under an atmosphere of purified argon in a MBraun Labmaster glovebox or using standard Schlenk techniques. MeCN and CH_2Cl_2 were dried over CaH_2, EtOH was dried over magnesium, and Et_2O and THF were dried over Na/K alloy and toluene over sodium. Benzene-d_6 and toluene-d_8 were distilled from Na/K alloy. Other deuterated solvents, such as CD_2Cl_2 and $CDCl_3$ were dried over 3 or 4 Å molecular sieves.

$FeCl_2$, $FeBr_2$, methyl benzoate, and $NaBH_4$ were purchased from Sigma-Aldrich and used as received. R-PN^{H}P (R = Et, ^{i}Pr, Cy, Ph, ^{t}Bu)[3,76−78] and amides[65,79] were prepared according to literature procedures. Complexes **1b** and **2b**, as well as the spectroscopic data for **4b** and **5b** have previously been reported.[16,18,21,27] ^{1}H, ^{13}C, ^{31}P, and ^{11}B NMR spectra were recorded using Bruker DRX 400, DRX 500 and Avance 500 NMR spectrometers. ^{1}H and ^{13}C{^{1}H}, and ^{13}C-APT (attached proton test) NMR chemical shifts are reported in ppm downfield from tetramethylsilane. The resonance of the residual protons in the deuterated solvent were used as internal standard for ^{1}H NMR spectroscopy. The solvent peak of the deuterated solvent was used as internal standard for ^{13}C NMR spectroscopy. Provided that the complexes exhibit sufficient stability, assignments in the ^{1}H and ^{13}C NMR data are based on ^{1}H-COSY, ^{1}H-NOESY, ^{1}H,^{13}C-HSQC, and ^{1}H,^{13}C-HMBC NMR spectroscopy and selective ^{31}P- and ^{11}B-decoupling experiments. ^{31}P NMR chemical shifts are reported in ppm downfield from H_3PO_4 and referenced to an external 85% solution of phosphoric acid in D_2O. ^{11}B NMR chemical shifts are reported in ppm downfield from $BF_3{\cdot}Et_2O$ and referenced to an external solution of $BF_3{\cdot}Et_2O$ in $CDCl_3$. The following abbreviations and combinations thereof are used for the description of NMR data: br (broad), s (singlet), d (doublet), t (triplet), q (quartet), quin (quintet), m (multiplet), and v (virtual).

FT-IR spectra were recorded by attenuated total reflection of the solid samples on a Bruker Tensor IF37 spectrometer. The intensity of the absorption band is indicated as vw (very weak), w (weak), m (medium), s (strong), vs (very strong), and br (broad).

HR-ESI mass spectra were acquired with a LTQ-FT mass spectrometer (Thermo Fisher Scientific). HR-APCI mass spectra were acquired with a LTQ-FT mass spectrometer (Thermo Fisher Scientific). In both cases, the resolution was set to 100.000. Elemental analyses were performed on a Vario Micro Cube Elemental Analyzer.

X-ray Crystallography. The single crystal X-ray diffraction data for the structural analysis has been collected using graphite-monochromated Mo−K_α-radiation ($\lambda_{MoK\alpha}$ = 0.71073 Å) on the imaging plate detector systems STOE IPDS2 (**1a**, **3c**, and **7c**) or on the pixel detector system BRUKER D8 QUEST (**1d**, **8c**, and **10e**). The structures were solved by direct methods with SHELXS-97 and refined against F^2 by full-matrix-least-squares techniques using SHELXL-97.[80] On the basis of the crystal descriptions, numerical absorption corrections were applied.[80,81] Crystallographic data for **1a**, **1d**, **3c**, **7c**, **8c**, and **10e** have been deposited at Cambridge Crystallographic Data Centre (CCDC 1449037-1449042) and can be obtained free of charge via www.ccdc.cam.ac.uk/. Details of the data collection and the refinement can be found in the Supporting Information.

*Synthesis of [(Et-PN^{H}P)Fe(Br)$_2$(CO)] (**1a**).* 393 mg (1.58 mmol, 1.00 equiv) of Et-PN^{H}P and 340 mg (1.58 mmol, 1.00 equiv) of $FeBr_2$ were suspended in 10 mL of THF. After stirring for 10 min, the argon

DOI: 10.1021/acs.organomet.6b00251
Organometallics XXXX, XXX, XXX−XXX

atmosphere in the Schlenk tube was replaced by 1 atm of CO, and stirring was continued for 10 min. Twenty milliliters of *n*-hexane was added, and the blue solution was stored for 16 h at −25 °C. After removing the colorless solution, the residue was dissolved in 15 mL of chloroform, and the solution was filtrated. After removal of the solvent and drying under vacuum, **1a** can be obtained as a blue solid. Yield: (524 mg, 1.06 mmol, 67%). Analysis calculated for $C_{13}H_{29}Br_2FeNOP_2$ (M = 492.98 g/mol): C, 31.67%; H, 5.93%; N, 2.84%. Found: C, 31.78%; H, 5.90%; N, 2.79%. ^{1}H NMR (300 MHz, CD_2Cl_2, 27 °C) δ: 1.32 (vsext, 12H, $^3J_{H-H}$ = 6.2 Hz, PCH_2CH_3), 2.09−2.24 (m, 10H, 2H NCH_2CH_2P + 8H PCH_2CH_3), 2.31−2.39 (m, 2H, NCH_2CH_2P), 3.21−3.34 (m, 2H, NCH_2CH_2P), 3.53−3.58 (m, 2H, NCH_2CH_2P), 4.74 (br, 1H, N*H*) ppm. ^{13}C{^{1}H} NMR (75 MHz, CD_2Cl_2, 27 °C) δ: 8.1 (s, PCH_2CH_3), 8.3 (s, PCH_2CH_3), 16.2 (vq, $^1J_{P-C}$ = 13.1 Hz, PCH_2CH_3), 28.0 (vt, $^1J_{P-C}$ = 8.7 Hz, NCH_2CH_2P), 50.0 (vt, $^2J_{P-C}$ = 4.6 Hz, NCH_2CH_2P). ^{31}P{^{1}H} NMR (122 MHz, CD_2Cl_2, 27 °C) δ = 64.3 (s) ppm. HR-MS (APCI+): *m*/*z* calcd 384.0304 [(Et-PN^{H}P)Fe(Br)]$^+$; found, 384.0318. FT-IR: $\tilde{\nu}$ [cm^{-1}] = 3182 (w, NH), 2964 (m), 2935 (m), 2910 (m), 2874 (m), 2162 (w), 2036 (w), 1936 (s, CO), 1892 (m), 1461 (m), 1450 (m), 1413 (m), 1380 (m), 1305 (w), 1249 (m), 1235 (m), 1209 (m), 1174 (m), 1125 (m), 1068 (s), 1040 (s), 1029 (s), 983 (m), 972 (m), 954 (w), 868 (m), 830 (m), 787 (w), 762 (s), 736 (m), 720 (s), 693 (s), 684 (s), 629 (s), 585 (s), 568 (s), 546 (s), 510 (w), 490 (w), 415 (m).

*Synthesis of [(Ph-PN^{H}P)Fe(Br)$_2$(CO)] (**1d**).* 800 mg (1.81 mmol, 1.00 equiv) Ph-PN^{H}P and 390 mg (1.81 mmol, 1.00 equiv) $FeBr_2$ were suspended in 60 mL of THF. After stirring for 1 h, the argon atmosphere in the Schlenk tube was replaced by 1 atm of CO, and stirring was continued for 3 h. After evaporation of the solvent, the purple residue was suspended in 5 mL of THF and filtered over silica. After washing with 3 × 5 mL THF, the product can be washed out of the frit with 3 × 10 mL of DCM. After removal of the solvent and drying under vacuum, **1d** can be obtained as a red solid, containing a mixture of *trans* and *cis* isomers. Complex **1d** is moderately stable in the solid state but reacts under loss of the CO ligand in solution, yielding the paramagnetic dibromo complex. Yield: 120 mg (0.18 mmol, 10%). $C_{29}H_{30}Br_2FeNOP_2$ (M = 686.16 g/mol). Because of the limited stability of **1d**, it was not possible to obtain an elemental analysis. ^{1}H NMR (300 MHz, $CDCl_3$, 27 °C) δ: 0.72−0.98 (m, 1H, CH_2), 1.93−2.16 (m, 1H, CH_2), 2.31−2.55 (m, 1H, CH_2), 2.63−3.15 (m, 3H, CH_2), 3.29−3.51 (m, 2H, CH_2), 3.53−3.71 (m, 1H, CH_2), 5,06 (t, 1H, $^2J_{PH}$ = 12.9 Hz, NH), 7.32−7.51 (m, 10H, Ph-*H*), 7.54−7.71 (m, 3H, Ph-*H*), 7.78−8.06 (m, 5H, Ph-*H*), 8.11−8.30 (m, 2H, Ph-*H*) ppm. ^{31}P{^{1}H} NMR (161.9 MHz, CD_2Cl_2, 27 °C) δ: 70.4 (s, *trans*-**1d**), 42.4 (s, *cis*-**1d**) ppm. Only the resonances which are changing upon ^{31}P-decoupling are listed in the following. ^{1}H{^{31}P} NMR (400 MHz, CD_2Cl_2, 27 °C, o2p = 71 ppm) δ: 3.46 (d, 2H, J_{HH} = 13.4 Hz, CH_2), 5.06 (s br, 1H, NH), 7.69 (d, 2H, $^3J_{HH}$ = 6.7 Hz, Ph-*H*), 7.95 (d, 2H, $^3J_{HH}$ = 5.8 Hz, Ph-*H*) ppm. ^{13}C-APT NMR (100.6 MHz, CD_2Cl_2, 27 °C): δ = 28.0 (d, $^1J_{PC}$ = 34.9 Hz, PCH_2), 50.5 (s, NCH_2), 128.0 (s, Ph-*C*), 128.3 (d, J_{PC} = 4.9 Hz, Ph-*C*), 128.8 (s, Ph-*C*), 129.2 (s, Ph-*C*), 130.0 (d, J_{PC} = 19.9 Hz, Ph-*C*), 130.4 (s, Ph-*C*), 131.0 (s, Ph-*C*), 131.5 (s, Ph-*C*), 132.9 (s, Ph-*C*), 134.1 (s, Ph-*C*) ppm. Because of the limited stability of **1d** in solution and the accompanying formation of paramagnetic compounds, quaternary carbon atoms could not be detected. MS (ESI+): *m*/*z* (%) = 442.3 (100) (Ph-PN^{H}P)H$^+$; 576.2 (75) [(Ph-PN^{H}P)Fe(Br)]$^+$. FT-IR: $\tilde{\nu}$ [cm^{-1}] = 3172 (w, NH), 3050 (w), 2934 (w), 2873 (w), 2360 (w), 2342 (w), 1940 (s, CO), 1916 (m, CO), 1587 (w), 1573 (w), 1484 (w), 1462 (w), 1434 (m), 1409 (w), 1333 (w), 1312 (w), 1275 (w), 1247 (w), 1212 (w), 1189 (w), 1171 (w), 1161 (w), 1098 (m), 1073 (w), 1055 (m), 1027 (w), 999 (w), 963 (m), 833 (m), 783 (w), 756 (m), 744 (s), 715 (m), 695 (s), 676 (m), 667 (m), 617 (w), 595 (w), 580 (m), 570 (m), 557 (m), 536 (s), 507 (s), 498 (s), 474 (m), 444 (m), 433 (m), 414 (m).

*Synthesis of [(Et-PN^{H}P)Fe(H)(CO)(BH$_4$)] (**2a**).* 400 mg (0.81 mmol) of [(Et-PN^{H}P)$FeBr_2$(CO)] (**1a**) was dissolved in 20 mL of EtOH. 153 mg (4.06 mmol, 5.10 equiv) of $NaBH_4$ was added in one portion, and the resulting yellow solution was stirred for 30 min. All volatiles were removed *in vacuo*, and the residue was extracted with 20 mL of toluene to give a yellow solution. The solution was filtrated over silica and stirred for 16 h. After removal of all volatiles, complex **2a** was obtained as a dark yellow solid. Despite several attempts with different crystallization methods and different solvents, it was not possible to grow suitable single crystals for X-ray diffraction. Yield: 266 mg (0.76 mmol, 94%). Analysis calculated for $C_{13}H_{35}BFeNOP_2$ (M = 350.03 g/mol): C 44.74%, H 9.82%, N 4.01%. Found: C 43.79%, H 9.62%, N 4.12%. ^{1}H NMR (500 MHz, C_6D_6, 27 °C) δ: −19.8 (t, 1 H, $^2J_{P-H}$ = 49.7 Hz, Fe*H*), −3.01 (s, br, 4H, BH_4), 0.98 (vquin, 6H, $^3J_{H-H}$ = 7.6 Hz, 2 x PCH_2CH_3), 1.49−1.40 (m, 4H, 2H NCH_2CH_2P + 2H PCH_2CH_3), 1.19 (vquin, 6H, $^3J_{H-H}$ = 7.7 Hz, 2 x PCH_2CH_3), 1.73−1.67 (m, 2H, NCH_2CH_2P), 1.56−1.50 (m, 4H, 2H NCH_2CH_2P + 2H PCH_2CH_3), 1.98−1.89 (m, 2H, PCH_2CH_3), 2.23−2.17 (m, 2H, PCH_2CH_3), 2.54−2.43 (m, 2H, NCH_2CH_2P), 3.79 (s, br, 1H, N*H*) ppm. ^{13}C{^{1}H} NMR (75 MHz, C_6D_6, 27 °C) δ: 8.5 (s, PCH_2CH_3), 20.3 (vt, $^1J_{P-C}$ = 11.1, PCH_2CH_3), 9.0 (s, PCH_2CH_3), 23.3 (vt, $^1J_{P-C}$ = 13.9, PCH_2CH_3), 28.1 (vt, $^1J_{P-C}$ = 8.4, NCH_2CH_2P), 53.3 (vt, $^2J_{P-C}$ = 6.2 Hz, NCH_2CH_2P) ppm. ^{11}B{^{1}H} NMR (160 MHz, C_6D_6, 27 °C) δ: −33.0 (s) ppm. ^{31}P{^{1}H} NMR (122 MHz, C_6D_6, 27 °C) δ: 81.3 (s) ppm. ^{31}P NMR (122 MHz, C_6D_6, 27 °C) δ: 81.4 (d, $^2J_{P-H}$ = 45.5 Hz) ppm. HR-MS (ESI+, MeOH/MeCN): calcd 334.1147 [(Et-PN^{H}P)-Fe(H) (CO)]$^+$; found, 334.1147; calcd, 375.1412 [(Et-PN^{H}P)Fe(H) (CO) (MeCN)]$^+$; found, 375.4107. FT-IR: $\tilde{\nu}$ [cm^{-1}] = 3201 (w, NH), 2962 (m), 2934 (w), 2906 (w), 2877 (w), 2383 (w, BH), 2351 (w, BH), 2347 (w, BH), 2300 (w, BH), 2050 (br), 1892 (s, CO), 1854 (m), 1833 (m), 1459 (m), 1412 (w), 1378 (w), 1306 (w), 1260 (s), 1207 (w), 1173 (w), 1065 (s), 1014 (s), 967 (w), 955 (m), 865 (w), 834 (m), 792 (vs), 762 (m), 731 (m), 712 (m), 689 (m), 629 (m), 602 (m), 558 (w), 495 (w), 424 (w).

*Formation of [(Et-PN^{H}P)Fe(H)$_2$(CO)] (**4a**) and [(Et-PNP)Fe(H)(CO)] (**5a**).* When a solution of complex **2a** in C_6D_6 was heated to 70 °C under ten atmospheres of hydrogen in a Fischer−Porter tube and is transferred after 1 h to an NMR tube, the ^{1}H and ^{31}P{^{1}H} NMR spectra of the mixture indicate a low conversion of complex **2a**. However, in the presence of an amide virtually complete conversion and the formation of complex **5a** as the major product is observed in addition to unidentified byproducts. A more selective reaction, however, is observed in the presence of BH_3-acceptors such as PEt_3, allowing for the detection of both the dihydride complexes **4a** and the *penta*-coordinated complex **5a**. The ^{31}P{^{1}H} NMR spectrum clearly indicated the formation of $Et_3P{\cdot}BH_3$ by a quartet at 22.05 ppm ($^1J_{PB}$ = 58.1 Hz) after 30 min. The ^{1}H NMR spectrum of the mixture gives rise to a multiplet resonance at −9.66 ppm is, which is assigned to *trans*-[(Et-PN^{H}P)Fe(H)$_2$(CO)] (*trans*-**4a**, δ_P = 93.1 ppm). A singlet resonance at 4.47 ppm in the ^{1}H NMR spectrum indicates the concomitant formation of elemental hydrogen in this reaction. Furthermore, minor quantities of the corresponding *cis*-isomer *cis*-**4a** (δ_H = −20.00 (td, $^2J_{PH}$ = 51.3 Hz, $^2J_{HH}$ = 14.2 Hz, Fe−*H*), −8.06 (td, $^2J_{PH}$ = 85.2 Hz, $^2J_{HH}$ = 14.9 Hz, Fe−*H*) ppm; δ_P = 87.5 ppm) and the *penta*-coordinated complex **5a** (δ_H = −24.40 (t, $^2J_{PH}$ = 50.9 Hz, Fe−*H*); δ_P = 78.0 ppm) were detected by ^{1}H and ^{31}P{^{1}H} NMR spectroscopy.

*Synthesis of [(Cy-PN^{H}P)Fe(H)(CO)(BH$_4$)] (**2c**).* 150 mg (0.32 mmol, 1.00 equiv) Cy-PN^{H}P and 108 mg (0.32 mmol, 1.00 equiv) $[Fe(H_2O)_6](BF_4)_2$ are dissolved in 8 mL of MeCN to yield an intense red solution (δ_p = 55.5 ppm). A solution of 183 mg (4.83 mmol, 15.0 equiv) of $NaBH_4$ in 8 mL of ethanol was added to the red solution, causing immediate gas evolution (δ_p = 80.1 ppm). The resulting orange solution was stirred for 1 h, after which the argon atmosphere was replaced by CO (1 atm), and the mixture was stirred for an additional 2 h (δ_p = 89.0 ppm). After evaporation of all volatiles, the residue was extracted with 3 × 10 mL *n*-hexane. A ^{31}P{^{1}H} NMR spectrum of the reaction mixture confirms the formation of complex **2c** together with approximately 50% of **3c**, which can be removed by precipitation and washing. The yellow solution was concentrated to a volume of 5 mL and cooled to −20 °C, which causes the precipitation of a light yellow solid. After separation of the supernatant solution, the solid was washed again with 5 mL of *n*-hexane at −20 °C and dried *in vacuo* to yield 60 mg (0.100 mmol, 31%) of **2c** as a yellow powder. ^{1}H NMR (400.0 MHz, C_6D_6, 27 °C) δ: −19.59 (t, $^2J_{PH}$ = 50.4 Hz, 1H, Fe-*H*), −2.84 (br, 4H, BH_4), 0.60−2.34 (m, 44H, Cy-*H*+3xCH_2), 2.56

DOI: 10.1021/acs.organomet.6b00251
Organometallics XXXX, XXX, XXX−XXX

(m, 4H, CH_2+Cy-*H*), 2.86 (m, 2H, Cy-*H*), 2.94 (m, 2H, Cy-*H*), 3.97 (m, 1H, N*H*) ppm. $^{31}P\{^1H\}$ NMR (161.9 MHz, C_6D_6, 27 °C) δ: 91.9 (s) ppm. $^{11}B\{^1H\}$ NMR (128.3 MHz, C_6D_6, 27 °C) δ: −31.4 (br) ppm. Only the resonances which are changing upon ^{31}P- or ^{11}B-decoupling are listed in the following. $^1H\{^{31}P\}$ NMR (400 MHz, CD_2Cl_2, 27 °C, o2p = 92 ppm) δ: −19.59 (s, 1H, Fe-*H*) ppm. ^{13}C-APT NMR (100.6 MHz, C_6D_6, 27 °C) δ: 16.7 (s, Cy-*C*), 20.2 (d, $^2J_{PC}$ = 29.4 Hz, Cy-*C*), 26.9 (s, Cy-*C*), 27.2 (s, Cy-*C*), 27.3 (s, Cy-*C*), 27.4 (s, Cy-*C*), 27.9 (s, Cy-*C*), 28.2 (s, Cy-*C*), 28.4 (s, Cy-*C*), 29.3 (s, Cy-*C*), 30.5 (s, Cy-*C*), 31.5 (s, Cy-*C*), 32.4 (d, $^1J_{P-C}$ = 32.4 Hz, *C*H), 36.8 (t, $^1J_{P-C}$ = 12.2 Hz, *C*H), 40.3 (t, $^1J_{P-C}$ = 8.9 Hz, *C*H), 45.0 (s, Cy-*C*), 54.4 (s, CH_2), 222.4 (dt, $^2J_{P-C}$ = 25.6 Hz, $^2J_{H-C}$ = 19.2 Hz, CO) ppm. MS (ESI+): *m*/*z* (%) = 522.7 (100) [(Cy-PN^{H}P)Fe(H)]$^+$; 550.5 (43) [(Cy-PN^{H}P)Fe(H) (CO)]$^+$; 590.8 (52) {[(Cy-PN^{H}P)Fe(H) (BH_4) (CO)]+Na}$^+$. HR-MS (ESI+): *m*/*z* calcd 550.3025 [(Cy-PN^{H}P)Fe-(H) (CO)]$^+$; found: 550.3035. FT-IR: $\tilde{\nu}$ [cm^{-1}] = 3467 (br), 3199 (w, NH), 2925(m), 2850 (m), 2361 (m, BH), 1900 (s, CO), 1821 (w), 1621 (w), 1447 (m), 1407 (w), 1343 (w), 1298 (w), 1270 (w), 1201 (w), 1176 (w), 1120 (w), 1067 (m), 1006 (w), 980 (w), 960 (w), 615 (w), 890 (w), 854 (w), 832 (w), 785 (w), 742 (w), 709 (w), 686 (w), 600 (w), 535 (w), 513 (w), 465 (w).

Analytical Data for ***3c.*** ^1H NMR (300 MHz, C_6D_6, 27 °C) δ: 0.90−1.07 (m br, 12H, Cy-*H* + BH_3), 1.13−1.71 (m, 34H, $^2J_{PH}$ = 13.8 Hz PBH_3), 1.72−1.88 (m br, 4H, Cy-H), 1.90−2.13 (m, 4H, NCH_2CH_2P), 2.94−3.18 (m, 4H, NCH_2CH_2P), 4.83 (br s, 1H, N*H*) ppm. Only the resonances which are changing upon ^{11}B-decoupling are listed in the following. $^1H\{^{11}B\}$ NMR (300 MHz, C_6D_6, 27 °C) δ: 1.08 (d, 6H, $^2J_{PH}$ = 13.8 Hz, PBH_3) ppm. $^{13}C\{^1H\}$ NMR (75 MHz, C_6D_6, 27 °C) δ: 14.0 (d, $^2J_{CP}$ = 30.3 Hz), 24.1 (s, *p*-Cy), 24.7 (vt, $^2J_{CP}$ = 2.2 Hz, *o*-Cy), 24.8 (s, *m*-Cy), 25.0 (s, *m*-Cy), 30.1 (d, $^1J_{CP}$ = 27.7 Hz, ipso-Cy), 30.5 (d, $^1J_{CP}$ = 27.5 Hz, ipso-Cy), 50.6 (s, NCH_2CH_2P) ppm. $^{31}P\{^1H\}$ NMR (122 MHz, C_6D_6, 27 °C) δ: 23.7 (br) ppm. $^{11}B\{^1H\}$ NMR (96 MHz, C_6D_6, 27 °C) δ: −43.0 (br) ppm. MS (ESI+): *m*/*z* (%) = 480.8 (45) [(Cy-PN^{H}P)·(BH_3)]H$^+$; 494.8 (100) [(Cy-PN^{H}P)·(BH_3)$_2$]H$^+$. HR-MS (ESI+): *m*/*z* calcd: 494.4391 [(Cy-PN^{H}P)·(BH_3)$_2$]H$^+$; found, 494.4388.

Formation of [(Ph-PN^{H}P)Fe(H)(CO)(BH_4)] ***(2d).*** 100 mg (0.23 mmol) of Ph-PN^{H}P and 49 mg (0.23 mmol, 1.00 equiv) of $FeBr_2$ are dissolved in 8 mL of MeCN to yield a red solution (δ_p = 64.9 ppm). A solution of 183 mg (4.83 mmol, 15.0 equiv) of $NaBH_4$ in 8 mL of ethanol is added, resulting in immediate gas evolution. After stirring for 1 h (δ_p = 83.4 ppm), the argon atmosphere was replaced by 1 atm CO, and the solution was stirred for two additional hours, leading to an orange solution. The solvent was evaporated, and the orange residue was extracted with 3 × 10 mL of toluene. After evaporation of the solvent, the residue was washed with 4 × 3 mL ethanol and dried under vacuum to yield a red solid, containing **2d** and **3d** according to $^{31}P\{^1H\}$ NMR spectroscopy. Because of the low stability of complex **2d**, all attempts to further purify this compound resulted in decomposition. ^1H NMR (400.0 MHz, CD_2Cl_2, 27 °C) δ: −18.13 (t, 1H, $^2J_{PH}$ = 52.3 Hz, Fe−*H*), −3.61 (br, 4H, BH_4), 2.39−2.54 (m, 2H, CH_2), 2.65−2.80 (m, 2H, CH_2), 2.90−3.06 (m, 2H, CH_2), 3.42−3.60 (m, 2H, CH_2), 4.26 (m, 1H, N*H*), 7.35−7.55 (m, 12H, Ph-*H*), 7.68−7.85 (m, 8H, Ph-*H*) ppm. $^{31}P\{^1H\}$ NMR (161.9 MHz, CD_2Cl_2, 27 °C) δ: 81.7 (s) ppm. $^{11}B\{^1H\}$ NMR (128.3 MHz, CD_2Cl_2, 27 °C) δ: −32.9 (br) ppm.

NMR Data for ***3d.*** ^1H NMR (300 MHz, C_6D_6, 27 °C) δ: 2.03−2.18 (m, 4H, NCH_2CH_2P), 2.86−3.02 (m, 4H, NCH_2CH_2P), 6.87−7.85 (m superimposed, 20H, phenyl-*H*) ppm. Only the resonances which are changing upon ^{11}B-decoupling are listed in the following. $^1H\{^{11}B\}$ NMR (300 MHz, C_6D_6, 27 °C) δ: 1.73 (d, 6H, $^2J_{PH}$ = 14.6 Hz, PBH_3) ppm. $^{31}P\{^1H\}$ NMR (202.5 MHz, C_6D_6, 27 °C) δ: 14.2 (br) ppm. $^{11}B\{^1H\}$ NMR (160.5 MHz, C_6D_6, 27 °C) δ: −40.5 (br) ppm.

The decomposition of complex **2d** in solution was monitored by ^1H and $^{31}P\{^1H\}$ NMR spectroscopy. Two superimposed triplet of doublet resonances in the ^1H NMR spectrum were assigned to the two hydrido ligands of the *trans*-dihydride complex **4d**, differing in the relative orientation of the amine proton in **4d**. Assignable NMR data of **4d**: ^1H NMR (400.0 MHz, C_6D_6, 27 °C) δ −8.55 (td superimposed, 1H, $^2J_{PH}$ = 44.8 Hz, $^2J_{HH}$ = 10.2 Hz, Fe-*H*), −8.45 (td superimposed, 1H, $^2J_{PH}$ = 62.9 Hz, $^2J_{HH}$ = 9.7 Hz, Fe-*H*) ppm. $^{31}P\{^1H\}$ NMR (162 MHz, C_6D_6, 27 °C) δ: 94.4 (s) ppm.

Formation of [(^{t}*Bu-PN^{H}P)Fe(H)(CO)(BH_4)]* ***(2e).*** 40 mg (0.11 mmol) of ^{t}Bu-PN^{H}P and 36 mg (0.11 mmol, 1.00 equiv) of $[Fe(H_2O)_6](BF_4)_2$ are mixed with 6 mL of MeCN, leading to a pale yellow solution and small amounts of a white precipitate. The mixture is cooled to −42 °C, resulting in a pale blue solution, and a solution of 60 mg (1.56 mmol, 30.0 equiv) of $NaBH_4$ in EtOH was added dropwise. After 1 h of stirring at −42 °C, a greenish yellow solution was formed. The argon atmosphere was replaced by 1 atm of carbon monoxide, and the mixture was stirred for a further 2 h at −42 °C, again leading to a color change and the formation of an intense orange solution. After this period, the mixture was allowed to warm to ambient temperature, all volatiles were removed *in vacuo*, and the orange residue was extracted with *n*-hexane and toluene. The $^{31}P\{^1H\}$ NMR spectrum of the extracted solutions indicates the presence of up to four species in addition to complex **2e**, including **3e**, **6e**, and **7e**. All attempts of purification or separation resulted in the decomposition of **2e**. Furthermore, complex **2e** turns out to be fairly unstable in solution and is only detectable for a couple of hours in solutions of the obtained mixtures. ^1H NMR (400.0 MHz, C_6D_6, 27 °C) δ: −20.83 (t, 1H, $^2J_{PH}$ = 60.2 Hz, Fe-*H*), −2.05 (br, 4H, BH_4), 1.16 (d, 18H, $^3J_{PH}$ = 9.7 Hz, $C(CH_3)_3$), 1.39 (d, 9H, $^3J_{PH}$ = 12.2 Hz, $C(CH_3)_3$), 1.41 (d, 9H, $^3J_{PH}$ = 11.0 Hz, $C(CH_3)_3$), 1,61 (m superimposed, 2H, CH_2), 2.02 (m superimposed, 2H, CH_2), 2.54 (br, 2H, CH_2), 2.95 (br, 2H. CH_2), 5.50 (br superimposed, 1H, N-*H*) ppm. $^{31}P\{^1H\}$ NMR (162 MHz, C_6D_6, 27 °C) δ: 111.0 (s) ppm. $^{11}B\{^1H\}$ NMR (128 MHz, C_6D_6, 27 °C) δ: −40.6 (br) ppm. Only the resonances which are changing upon ^{31}P- or ^{11}B-decoupling are listed in the following. $^1H\{^{31}P\}$ NMR (400.0 MHz, C_6D_6, 27 °C, o2p = 111.0 ppm) δ: −20.83 (s, 1H, Fe-*H*), 1.16 (s, 18H, $C(CH_3)_3$), 1.39 (s, 9H, $C(CH_3)_3$), 1.41 (s, 9H, $C(CH_3)_3$) ppm.

NMR Data for ***3e.*** ^1H NMR (300 Hz, C_6D_6, 27 °C) δ: 0.98 (d, 18H, $^3J_{PH}$ = 9.5 Hz $C(CH_3)_3$), 1.03 (d, 18H, $^3J_{PH}$ = 9.6 Hz $C(CH_3)_3$), 2.00−2.13 (m, 4H, NCH_2CH_2P), 3.04−3.17 (m, 4H, NCH_2CH_2P), 4.90 (br s, 1H, N*H*) ppm. Only the resonances which are changing upon ^{11}B-decoupling are listed in the following. $^1H\{^{11}B\}$ NMR (300 Hz, C_6D_6, 27 °C) δ: 1.04 (d, 6H, $^2J_{P-H}$ = 12.8 Hz, PBH_3), ppm. $^{13}C\{^1H\}$ NMR (75 MHz, C_6D_6, 27 °C) δ: 15.0 (d, $^1J_{C-P}$ = 28.3 Hz, NCH_2CH_2P), 27.6 (s, CCH_3), 53.7 (d, $^2J_{C-P}$ = 2.9 Hz, CCH_3), 63.3 (s, NCH_2CH_2P) ppm. $^{31}P\{^1H\}$ NMR (160 MHz, C_6D_6, 27 °C) δ: 41.9 (br) ppm. $^{11}B\{^1H\}$ NMR (122 MHz, C_6D_6, 27 °C) δ: −42.5 (br) ppm.

NMR Data for ***6e.*** $^{31}P\{^1H\}$ NMR (162 MHz, C_6D_6, 27 °C) δ: 103.7 (br) ppm. $^{11}B\{^1H\}$ NMR (128 MHz, C_6D_6, 27 °C) δ: −21.9 (br) ppm. ^1H NMR (400.0 MHz, C_6D_6, 27 °C) δ: −15.85 (t, 1H, $^2J_{PH}$ = 63.4 Hz, Fe-*H*), −10.30 (br, 1H, Fe-*H*B), 1.21 (superimposed, $C(CH_3)_3$), 1.40 (superimposed, $C(CH_3)_3$), 1.61 (m, 2H, CH_2), 2.08 (m, 2H, CH_2), 2.40 (m, 2H, CH_2), 3.12 (m, 2H, CH_2) ppm. The terminal B−H-resonance could not be assigned.

NMR Data for ***7e.*** $^{31}P\{^1H\}$ NMR (162 MHz, C_6D_6, 27 °C) δ: 118.2 (AB-system, J_{AB} = 119.0 Hz, $\Delta\nu$ = 624.7 Hz) ppm. $^{11}B\{^1H\}$ NMR (128 MHz, C_6D_6, 27 °C) δ: −11.9, −42.5 (br) ppm. ^1H NMR (400.0 MHz, C_6D_6, 27 °C) δ: −14.93 (td, 1H, $^2J_{PH}$ = 59.4 Hz, $^3J_{HH}$ = 4.2 Hz, Fe-*H*), −9.65 (br, 1H, Fe-*H*B), 1.26 (superimposed, $C(CH_3)_3$), 1.37 (superimposed, $C(CH_3)_3$), 1.95 (m, CH_2), 2.12 (m, CH_2), 2.30 (m, CH_2), 2.76 (m, CH_2), 3.37 (m, CH_2), 3.77 (m, CH_2) ppm. Because of the complex structure of **7e**, it was not possible to assign all CH_2-, ^{t}Bu-, and B−H-resonances in the obtained mixtures.

Synthesis of [((Cy-PNP)BH_2N((CH_2)$_2$PCy_2BH_3)$_2$)FeH(CO)] ***(7c).*** 106 mg (0.23 mmol) of Cy-PN^{H}P and 77 mg (0.23 mmol, 1.00 equiv) of $[Fe(H_2O)_6](BF_4)_2$ are dissolved in 8 mL of MeCN, yielding an intense red solution. A solution of 130 mg (3.41 mmol, 15.0 equiv) of $NaBH_4$ in 8 mL of ethanol was added dropwise, which causes gas evolution. The resulting orange solution was stirred for 1 h, the argon atmosphere was replaced by CO (1 atm), and the mixture was stirred for 2 additional hours. After evaporation of the solvent, the residue was extracted with 3 × 10 mL *n*-hexane, and the yellow solution was concentrated to a volume of 10 mL. After stirring for 1 week, the solvent was evaporated, and the yellow residue was recrystallized from

DOI: 10.1021/acs.organomet.6b00251
Organometallics XXXX, XXX, XXX−XXX

diethyl ether. After drying *in vacuo*, the product was obtained as a yellow powder with an approximate yield of 60% (based on Cy-PN^{H}P). Crystals suitable for X-ray diffraction are obtained by recrystallizing from *n*-hexane at room temperature. ^{1}H NMR (300.1 MHz, C_6D_6) δ: −14.60 (td, 1H, $^2J_{PH}$ = 59.9 Hz, $^2J_{HH}$= 4.7 Hz, Fe-*H*), −11.17 (br, 1H, $\nu_{1/2}$ = 53.5 Hz, B*H*), 1.24 (d, 1H, $^2J_{HH}$ = 14.3 Hz, B-*H*-Fe), 0.79−2.17 (m, 98H, C*H*$_2$ + Cy-*H* + P−B*H*$_3$), 2.24 (m, 3H, Cy-*H*), 2.34 (br d, 1H, Cy-*H*), 2.66−2.77 (m, 2H, Cy-*H*), 2.89−2.98 (m, 1H, C*H*$_2$), 3.19 (br, 1H, BH), 3.40 (ddd, 2H, J_{PH} = 34.1 Hz, J_{HH} = 10.4 Hz, J_{HH} = 8.2 Hz, C*H*$_2$), 3.64 (ddd, 1H, J_{PH} = 34.1 Hz, J_{HH} = 11.2 Hz, J_{HH} = 7.8 Hz, C*H*$_2$) ppm. ^{31}P{^{1}H} NMR (161.9 MHz, C_6D_6) δ: 24.3 (br, *P*-BH$_3$), 97.8 (AB-system, J_{AB} = 118.6 Hz, $\Delta\nu$ = 963.7 Hz) ppm. ^{11}B{^{1}H} NMR (128 MHz, C_6D_6, 27 °C) δ: −11.8 (br, N-*B*-N), −42.6 (br, P-*B*H$_3$) ppm. Only the resonances which are changing upon ^{11}B-decoupling are listed in the following. ^{1}H{^{11}B} NMR (400.0 MHz, C_6D_6, 27 °C, o2p = −42.6 ppm) δ: −11.17 (br, 1H, $\nu_{1/2}$ = 21.4 Hz, B−H−Fe), 1.25 (d, 6H, $^2J_{PH}$ = 14.3 Hz, P−B*H*$_3$) ppm. ^{1}H{^{31}P} NMR (400.0 MHz, C_6D_6, 27 °C, o2p = 111.0 ppm) δ: −14.60 (d, 1H, $^2J_{HH}$ = 4.9 Hz, Fe-*H*), 2.24 (dd, 3H, J_{HH} = 12.0 Hz, J_{HH} = 5.8 Hz, Cy-*H*), 2.93 (q, 1H, J_{HH} = 7.0 Hz, C*H*$_2$), 3.40 (dd, 2H, J_{HH} = 10.3 Hz, J_{HH} = 8.2 Hz, C*H*$_2$), 3.64 (dd, 1H, J_{HH} = 11.1 Hz, J_{HH} = 7.8 Hz, C*H*$_2$) ppm. The terminal B−H-resonance could not be assigned. ^{13}C{^{1}H} NMR (125.8 MHz, C_6D_6, 27 °C,) δ: 15.2 (Cy-C), 19.5 (Cy-C), 22.9−33.3 (superimposed, Cy-C), 36.1 (Cy-*C*), 41.9 (Cy-C), 44.5 (C*H*$_2$), 45.5 (C*H*$_2$), 58.0 (C*H*$_2$), 60.6 (C*H*$_2$) ppm. The resonance of the coordinated carbonyl ligand was not observed. MS (ESI+): *m*/*z* (%) = 409.3 (34); 492.8 (35) [(Cy-PNP)·(BH$_3$)$_2$]$^+$; 528.6 (100); 560.5 (43); 574.9 (30); 1055.5 (16) [(Cy-PNP)Fe(H) (BH$_2$R) (CO)]$^+$. HR-MS (ESI+): *m*/*z* calcd 1055.7531 [(Cy-PNP)Fe(H) (BH$_2$R) (CO)]$^+$; found, 1055.7550. FT-IR: $\tilde{\nu}$ [cm^{-1}] = 2924 (s), 2851 (m), 2362 (m, BH), 2342 (m, BH), 1891 (m, CO), 1446 (m), 1409 (w), 1344 (w), 1260 (m), 1208 (w), 1173 (w), 1061(s), 1012 (s), 916 (w), 889 (w), 854 (m), 797 (s), 749 (m), 668 (w), 615(w), 588 (w), 511 (w), 464 (w).

Formation of [(Cy-PNP)BH$_2$NH-Ph)FeH(CO)] (**9c**). [(Cy-PN^{H}P)Fe-(H) (CO) (BH$_4$)] (**2c**, 30 mg, 0.05 mmol) was dissolved in 0.6 mL of C_6D_6 and placed in a J. Young NMR tube. Aniline (10 mg, 0.11 mmol, 2.20 equiv) was added, and the argon atmosphere was replaced by 1 atm of hydrogen. The mixture was heated to 50 °C and subsequently analyzed by NMR spectroscopy. ^{1}H NMR (400 MHz, C_6D_6, 27 °C) δ: −14.55 (t, 1H, J_{AB} = 119.0 Hz, Fe-*H*), −10.49 (br, 1H, Fe-*H*BH-N), 0.84−2.40 (superimposed m, 45H, Cy-H + CH2), 2.69 (superimposed, 2H, C*H*$_2$), 3.18 (d br, 2H, J_{PH} = 29.2 Hz, C*H*$_2$), 3.25 (br, 1H, Fe-HB*H*-N), 3.36 (dt, 2H, J_{PH} = 32.9 Hz, $^3J_{HH}$ = 8.5 Hz, C*H*$_2$), 3.62 (dt, 1H, J_{PH} = 32.9 Hz, $^3J_{HH}$ = 8.5 Hz, C*H*$_2$), 4.57 (br, 1H, B−N*H*-Ph), 6.80 (m, 3H, Ph-*H*), 7.32 (t, 2H, $^3J_{HH}$ = 7.3 Hz, Ph-*H*) ppm. ^{31}P{^{1}H} NMR (162 MHz, C_6D_6, 27 °C) δ: 101.3 (AB-system, J_{AB} = 118.6 Hz, $\Delta\nu$ = 199.7 Hz) ppm. ^{11}B{^{1}H} NMR (128 MHz, C_6D_6, 27 °C) δ: −16.2 (br) ppm.

■ ASSOCIATED CONTENT

Supporting Information

The Supporting Information is available free of charge on the ACS Publications website at DOI: 10.1021/acs.organomet.6b00251.

Crystallographic and spectroscopic details (PDF)
X-ray data (CIF)
X-ray data (CIF)
X-ray data (CIF)
X-ray data (CIF)
X-ray data (CIF)
X-ray data (CIF)

■ AUTHOR INFORMATION

Corresponding Author

*E-mail: robert.langer@chemie.uni-marburg.de.

Author Contributions

F.S. and M.A. contributed equally to this work.

Notes

The authors declare no competing financial interest.

■ ACKNOWLEDGMENTS

This research is supported by the DFG (LA 2830/3-1) and the NSFC (21450110063). R.L. is grateful to Professor S. Dehnen and Professor C. v. Hänisch for their continuous support and assistance.

■ REFERENCES

(1) Cornils, B.; Herrmann, W. A. *Applied Homogeneous Catalysis with Organometallic Compounds: A Comprehensive Handbook in Two Volumes*; Wiley-VCH: Weinheim, Germany, 1996.
(2) Khusnutdinova, J. R.; Milstein, D. *Angew. Chem., Int. Ed.* **2015**, *54*, 12236−12273.
(3) Schneider, S.; Meiners, J.; Askevold, B. *Eur. J. Inorg. Chem.* **2012**, *2012*, 412−429.
(4) Grützmacher, H. *Angew. Chem., Int. Ed.* **2008**, *47*, 1814−1818.
(5) Gunanathan, C.; Milstein, D. *Acc. Chem. Res.* **2011**, *44*, 588−602.
(6) Gunanathan, C.; Milstein, D. *Science* **2013**, *341*, 249−261.
(7) Liu, Q.; Wu, L.; Jackstell, R.; Beller, M. *Nat. Commun.* **2015**, *6*, 5933.
(8) Zell, T.; Langer, R. *Recycl. Catal.* **2016**, *2*, 87−109.
(9) Bauer, I.; Knölker, H. J. *Chem. Rev.* **2015**, *115*, 3170−3387.
(10) Morris, R. H. *Acc. Chem. Res.* **2015**, *48*, 1494−1502.
(11) Plietker, B. *Synlett* **2010**, *2010*, 2049−2058.
(12) Li, Y.-Y.; Yu, S.-L.; Shen, W.-Y.; Gao, J.-X. *Acc. Chem. Res.* **2015**, *48*, 2587−2598.
(13) Misal Castro, L. C.; Li, H.; Sortais, J.-B.; Darcel, C. *Green Chem.* **2015**, *17*, 2283−2303.
(14) Quintard, A.; Rodriguez, J. *Angew. Chem., Int. Ed.* **2014**, *53*, 4044−4055.
(15) Zell, T.; Milstein, D. *Acc. Chem. Res.* **2015**, *48*, 1979−1994.
(16) Alberico, E.; Sponholz, P.; Cordes, C.; Nielsen, M.; Drexler, H.-J.; Baumann, W.; Junge, H.; Beller, M. *Angew. Chem., Int. Ed.* **2013**, *52*, 14162−14166.
(17) Bielinski, E. A.; Förster, M.; Zhang, Y.; Bernskoetter, W. H.; Hazari, N.; Holthausen, M. C. *ACS Catal.* **2015**, *5*, 2404−2415.
(18) Bielinski, E. A.; Lagaditis, P. O.; Zhang, Y.; Mercado, B. Q.; Wurtele, C.; Bernskoetter, W. H.; Hazari, N.; Schneider, S. *J. Am. Chem. Soc.* **2014**, *136*, 10234−10237.
(19) Bonitatibus, P. J.; Chakraborty, S.; Doherty, M. D.; Siclovan, O.; Jones, W. D.; Soloveichik, G. L. *Proc. Natl. Acad. Sci. U. S. A.* **2015**, *112*, 1687−1692.
(20) Chakraborty, S.; Brennessel, W. W.; Jones, W. D. *J. Am. Chem. Soc.* **2014**, *136*, 8564−8567.
(21) Chakraborty, S.; Dai, H.; Bhattacharya, P.; Fairweather, N. T.; Gibson, M. S.; Krause, J. A.; Guan, H. *J. Am. Chem. Soc.* **2014**, *136*, 7869−72.
(22) Chakraborty, S.; Lagaditis, P. O.; Förster, M.; Bielinski, E. A.; Hazari, N.; Holthausen, M. C.; Jones, W. D.; Schneider, S. *ACS Catal.* **2014**, *4*, 3994−4003.
(23) Fairweather, N. T.; Gibson, M. S.; Guan, H. *Organometallics* **2015**, *34*, 335−339.
(24) Gorgas, N.; Stöger, B.; Veiros, L. F.; Pittenauer, E.; Allmaier, G.; Kirchner, K. *Organometallics* **2014**, *33*, 6905−6914.
(25) Lagaditis, P. O.; Sues, P. E.; Sonnenberg, J. F.; Wan, K. Y.; Lough, A. J.; Morris, R. H. *J. Am. Chem. Soc.* **2014**, *136*, 1367−1380.
(26) Sonnenberg, J. F.; Lough, A. J.; Morris, R. H. *Organometallics* **2014**, *33*, 6452−6465.
(27) Werkmeister, S.; Junge, K.; Wendt, B.; Alberico, E.; Jiao, H.; Baumann, W.; Junge, H.; Gallou, F.; Beller, M. *Angew. Chem., Int. Ed.* **2014**, *53*, 8722−8726.

DOI: 10.1021/acs.organomet.6b00251
Organometallics XXXX, XXX, XXX−XXX

(28) Zhang, Y.; MacIntosh, A. D.; Wong, J. L.; Bielinski, E. A.; Williard, P. G.; Mercado, B. Q.; Hazari, N.; Bernskoetter, W. H. *Chem. Sci.* **2015**, *6*, 4291−4299.
(29) Glüer, A.; Förster, M.; Celinski, V. R.; Schmedt auf der Günne, J.; Holthausen, M. C.; Schneider, S. *ACS Catal.* **2015**, *5*, 7214−7217.
(30) Sharninghausen, L. S.; Mercado, B. Q.; Crabtree, R. H.; Hazari, N. *Chem. Commun.* **2015**, *51*, 16201−4.
(31) Langer, R.; Diskin-Posner, Y.; Leitus, G.; Shimon, L. J. W.; Ben-David, Y.; Milstein, D. *Angew. Chem., Int. Ed.* **2011**, *50*, 9948−9952.
(32) Langer, R.; Iron, M. A.; Konstantinovski, L.; Diskin-Posner, Y.; Leitus, G.; Ben-David, Y.; Milstein, D. *Chem. - Eur. J.* **2012**, *18*, 7196−7209.
(33) Langer, R.; Leitus, G.; Ben-David, Y.; Milstein, D. *Angew. Chem., Int. Ed.* **2011**, *50*, 2120−2124.
(34) Zell, T.; Ben-David, Y.; Milstein, D. *Angew. Chem., Int. Ed.* **2014**, *53*, 4685−4689.
(35) Zell, T.; Ben-David, Y.; Milstein, D. *Catal. Sci. Technol.* **2015**, *5*, 822−826.
(36) Zell, T.; Butschke, B.; Ben-David, Y.; Milstein, D. *Chem. - Eur. J.* **2013**, *19*, 8068−8072.
(37) Bhattacharya, P.; Krause, J. A.; Guan, H. *Organometallics* **2011**, *30*, 4720−4729.
(38) Bhattacharya, P.; Krause, J. A.; Guan, H. *J. Am. Chem. Soc.* **2014**, *136*, 11153−11161.
(39) Harvey, J. N.; Poli, R. *Dalton Trans.* **2003**, 4100−4106.
(40) Ryther, R. J.; Weitz, E. *J. Phys. Chem.* **1991**, *95*, 9841−9852.
(41) Addison, A. W.; Rao, T. N.; Reedijk, J.; van Rijn, J.; Verschoor, G. C. *J. Chem. Soc., Dalton Trans.* **1984**, 1349−1356.
(42) Koehne, I.; Schmeier, T. J.; Bielinski, E. A.; Pan, C. J.; Lagaditis, P. O.; Bernskoetter, W. H.; Takase, M. K.; Würtele, C.; Hazari, N.; Schneider, S. *Inorg. Chem.* **2014**, *53*, 2133−2143.
(43) Mejuto, C.; Garcia-Eleno, M. A.; Guisado-Barrios, G.; Spasyuk, D.; Gusev, D.; Peris, E. *Org. Chem. Front.* **2015**, *2*, 936−941.
(44) Zell, T.; Langer, R.; Iron, M. A.; Konstantinovski, L.; Shimon, L. J. W.; Diskin-Posner, Y.; Leitus, G.; Balaraman, E.; Ben-David, Y.; Milstein, D. *Inorg. Chem.* **2013**, *52*, 9636−9649.
(45) Glatz, M.; Holzhacker, C.; Bichler, B.; Mastalir, M.; Stöger, B.; Mereiter, K.; Weil, M.; Veiros, L. F.; Mösch-Zanetti, N. C.; Kirchner, K. *Eur. J. Inorg. Chem.* **2015**, *2015*, 5053−5065.
(46) For details, please see Supporting Information.
(47) Bau, R.; Yuan, H. S. H.; Baker, M. V.; Field, L. D. *Inorg. Chim. Acta* **1986**, *114*, L27−L28.
(48) Marks, T. J.; Kolb, J. R. *Chem. Rev.* **1977**, *77*, 263−293.
(49) Binger, P.; Sandmeyer, F.; Krueger, C. *Organometallics* **1995**, *14*, 2969−2976.
(50) Fachinetti, G.; Floriani, C.; Mellini, M.; Merlino, S. *J. Chem. Soc., Chem. Commun.* **1976**, 300−301.
(51) Friedrich, A.; Drees, M.; Schneider, S. *Chem. - Eur. J.* **2009**, *15*, 10339−10342.
(52) Fryzuk, M. D.; MacKay, B. A.; Johnson, S. A.; Patrick, B. O. *Angew. Chem., Int. Ed.* **2002**, *41*, 3709−3712.
(53) Hillier, A. C.; Fox, T.; Schmalle, H. W.; Berke, H. *J. Organomet. Chem.* **2003**, *669*, 14−24.
(54) Jaska, C. A.; Temple, K.; Lough, A. J.; Manners, I. *Chem. Commun.* **2001**, 962−963.
(55) Jaska, C. A.; Temple, K.; Lough, A. J.; Manners, I. *J. Am. Chem. Soc.* **2003**, *125*, 9424−9434.
(56) Sloan, M. E.; Staubitz, A.; Clark, T. J.; Russell, C. A.; Lloyd-Jones, G. C.; Manners, I. *J. Am. Chem. Soc.* **2010**, *132*, 3831−3841.
(57) Stephens, F. H.; Pons, V.; Tom Baker, R. *Dalton Trans.* **2007**, 2613−2626.
(58) Wrackmeyer, B.; Molla, E.; Thoma, P.; Klimkina; Elena, V.; Tok; Oleg, L.; Bauer, T.; Kempe, R. *Z. Anorg. Allg. Chem.* **2011**, *637*, 401−405.
(59) Pelczar, E. M.; Emge, T. J.; Krogh-Jespersen, K.; Goldman, A. S. *Organometallics* **2008**, *27*, 5759−5767.
(60) Dub, P. A.; Ikariya, T. *ACS Catal.* **2012**, *2*, 1718−1741.
(61) Barrios-Francisco, R.; Balaraman, E.; Diskin-Posner, Y.; Leitus, G.; Shimon, L. J. W.; Milstein, D. *Organometallics* **2013**, *32*, 2973−2982.
(62) Coetzee, J.; Dodds, D. L.; Klankermayer, J.; Brosinski, S.; Leitner, W.; Slawin, A. M. Z.; Cole-Hamilton, D. J. *Chem. - Eur. J.* **2013**, *19*, 11039−11050.
(63) Ito, M.; Kobayashi, C.; Himizu, A.; Ikariya, T. *J. Am. Chem. Soc.* **2010**, *132*, 11414−11415.
(64) Ito, M.; Koo, L. W.; Himizu, A.; Kobayashi, C.; Sakaguchi, A.; Ikariya, T. *Angew. Chem., Int. Ed.* **2009**, *48*, 1324−1327.
(65) Ito, M.; Ootsuka, T.; Watari, R.; Shiibashi, A.; Himizu, A.; Ikariya, T. *J. Am. Chem. Soc.* **2011**, *133*, 4240−4242.
(66) Ito, M.; Sakaguchi, A.; Kobayashi, C.; Ikariya, T. *J. Am. Chem. Soc.* **2007**, *129*, 290−291.
(67) John, J. M.; Bergens, S. H. *Angew. Chem., Int. Ed.* **2011**, *50*, 10377−10380.
(68) John, J. M.; Takebayashi, S.; Dabral, N.; Miskolzie, M.; Bergens, S. H. *J. Am. Chem. Soc.* **2013**, *135*, 8578−8584.
(69) Kita, Y.; Higuchi, T.; Mashima, K. *Chem. Commun.* **2014**, *50*, 11211−3.
(70) Nuñez Magro, A. A.; Eastham, G. R.; Cole-Hamilton, D. J. *Chem. Commun.* **2007**, 3154−3156.
(71) Miura, T.; Held, I. E.; Oishi, S.; Naruto, M.; Saito, S. *Tetrahedron Lett.* **2013**, *54*, 2674−2678.
(72) Smith, A. M.; Whyman, R. *Chem. Rev.* **2014**, *114*, 5477−510.
(73) Werkmeister, S.; Junge, K.; Beller, M. *Org. Process Res. Dev.* **2014**, *18*, 289−302.
(74) During the review process, an iron-based catalyst has been reported for the hydrogenation of amides: Garg, J. A.; Chakraborty, S.; Ben-David, Y.; Milstein, D. *Chem. Commun.* **2016**, *52*, 5285−5288.
(75) Cantillo, D. *Eur. J. Inorg. Chem.* **2011**, *2011*, 3008−3013.
(76) Danopoulos, A. A.; Wills, A. R.; Edwards, P. G. *Polyhedron* **1990**, *9*, 2413−2418.
(77) Clarke, Z. E.; Maragh, P. T.; Dasgupta, T. P.; Gusev, D. G.; Lough, A. J.; Abdur-Rashid, K. *Organometallics* **2006**, *25*, 4113−4117.
(78) Meiners, J.; Friedrich, A.; Herdtweck, E.; Schneider, S. *Organometallics* **2009**, *28*, 6331−6338.
(79) Ohtaka, J.; Sakamoto, T.; Kikugawa, Y. *Tetrahedron Lett.* **2009**, *50*, 1681−1683.
(80) Sheldrick, G. *Acta Crystallogr., Sect. A: Found. Crystallogr.* **2008**, *64*, 112−122.
(81) *STOE X-Area 1.56 Program Package, Crystal Optimization for Numerical Absorption Correction Program*; Stoe & Cie GmbH: Darmstadt, Germany, 2011.
(82) During manuscript preparation the following manuscript was published: Elangovan, S.; Wendt, B.; Topf, C.; Bachmann, S.; Scalone, M.; Spannenberg, A.; Jiao, H.; Baumann, W.; Junge, K.; Beller, M. *Adv. Synth. Catal.* **2016**, *358*, 820−825.

DOI: 10.1021/acs.organomet.6b00251
Organometallics XXXX, XXX, XXX−XXX